



Transcription factor mediated control of anthocyanin biosynthesis in vegetative tissues

Outchkourov, N. S., Karlova, R. B., Hölscher, M., Schrama, X., Blilou, I., Jongedijk, E. J., ... Beekwilder, M. J.

This is a "Post-Print" accepted manuscript, which has been published in "Plant Physiology"

This version is distributed under a non-commercial no derivatives Creative Commons



(CC-BY-NC-ND) user license, which permits use, distribution, and reproduction in any medium, provided the original work is properly cited and not used for commercial purposes. Further, the restriction applies that if you remix, transform, or build upon the material, you may not distribute the modified material.

Please cite this publication as follows:

Outchkourov, N. S., Karlova, R. B., Hölscher, M., Schrama, X., Blilou, I., Jongedijk, E. J., ... Beekwilder, M. J. (2018). Transcription factor mediated control of anthocyanin biosynthesis in vegetative tissues. *Plant Physiology*. DOI: 10.1104/pp.17.01662

You can download the published version at:

<https://doi.org/10.1104/pp.17.01662>

1 **Anthocyanins on demand**

2 **Corresponding author:** *Correspondence to: J. Beekwilder; e-mail: jules.beekwilder@wur.nl, tel:
3 +31 317 480979, fax: +31 317 418094

4 **Transcription factor mediated control of anthocyanin biosynthesis in**
5 **vegetative tissues**

6

7 Nikolay S. Outchkourov^{1,a}, Rumyana Karlova^{2,a}, Matthijs Hölscher¹, Xandra Schrama¹, Ikram Blilou³,
8 Esmer Jongedijk², Carmen Diez Simon², Aalt D.J. van Dijk^{1,4,5}, Dirk Bosch¹, Robert D. Hall^{1,2}, Jules
9 Beekwilder^{1*}

10 ¹Wageningen Plant Research, Bioscience, PO Box 16, 6700 AA, Wageningen, The Netherlands

11 ²Wageningen University, Laboratory of Plant Physiology, Droevendaalsesteeg 1, 6708 PB The Netherlands

12 ³Wageningen University, Plant Developmental Biology, Droevendaalsesteeg 1, 6708 PB, The Netherlands

13 ⁴Wageningen University, Biometris, Droevendaalsesteeg 1, 6708 PB, Wageningen, The Netherlands

14 ⁵Wageningen University, Laboratory of Bioinformatics, Droevendaalsesteeg 1, 6708 PB, Wageningen, The Netherlands

15 ^a: these authors contributed equally to the manuscript

16

17 **LIST OF AUTHOUR CONTRIBUTIONS**

18

19 N.S.O. and R.K. performed most of the experiments with the help of M.H., X.S., E.J., I.B. and C.D.S.,
20 A.J.v.D. analysed the data, J.B., R.D.H. and D.B supervised the project, N.S.O., R.K. and J.B. wrote
21 the article together with the input from all the authors.

22

23

24 Funding information: NSO, RDH and JB were supported by the “Platform Green Synthetic Biology”
25 program 3, funded by the Netherlands Genomics Initiative. JB and RDH acknowledge support by the
26 EU 7th Framework ATHENA project (FP7-KBBE-2009-3-245121-ATHENA).

27

28

29

30

31

32 **SUMMARY**

33 Plants accumulate secondary metabolites to adapt to environmental conditions. These compounds,
34 here exemplified by the purple coloured anthocyanins, are accumulated upon high temperatures, UV-
35 light, drought and nutrient deficiencies, and may contribute to tolerance to these stresses. Producing
36 compounds is often part of a more broad response of the plant to changes in the environment. Here
37 we investigate how a transcription-factor mediated program for controlling anthocyanin biosynthesis
38 also has effects on formation of specialized cell structures and changes in the plant root architecture.
39 A systems biology approach was developed in tomato for coordinated induction of biosynthesis of
40 anthocyanins, in a tissue- and development independent manner. A transcription factor couple from
41 *Antirrhinum* that is known to control anthocyanin biosynthesis was introduced in tomato under control
42 of a dexamethasone-inducible promoter. By application of dexamethasone, anthocyanin formation
43 was induced within 24h in vegetative tissues and in undifferentiated cells. Profiles of metabolites and
44 gene expression were analysed in several tomato tissues. Changes in concentration of anthocyanins
45 and other phenolic compounds were observed in all tested tissues, accompanied by induction of the
46 biosynthetic pathways leading from glucose to anthocyanins. A number of pathways that are not
47 known to be involved in anthocyanin biosynthesis were observed to be regulated. Anthocyanin-
48 producing plants displayed profound physiological and architectural changes, depending on the tissue,
49 including root branching, root epithelial cell morphology, seed germination and leaf conductance. The
50 inducible anthocyanin-production system reveals a range of phenomena that accompany anthocyanin
51 biosynthesis in tomato, including adaptations of the plants architecture and physiology.

52

53

54 INTRODUCTION

55 Anthocyanins are abundant vacuolar pigments derived from the phenylpropanoid pathway and are
56 produced in many different plant species. Depending on the pH and their chemical modifications,
57 anthocyanins can change colour from red to purple and blue. Selecting for petal colour in ornamental
58 plants has been the subject of extensive research (Sasaki and Nakayama, 2015). This research has
59 revealed many different enzymes involved in chemical modifications such as glycosylation,
60 methylation and acylation of anthocyanins. While anthocyanins in flowers and fruits are known to
61 function as attractants for pollinators and vectors for seed dispersal, the role of anthocyanin
62 accumulation under stress in vegetative tissues is probably linked to the scavenging of reactive
63 oxygen species (Gould, 2004). In tomato, anthocyanins are predominantly found in stem and
64 hypocotyl tissues, as a result of stress conditions (Roldan et al., 2014).

65 Anthocyanins are powerful antioxidants and, as part of human diet in seeds, fruit and leaves
66 are proposed to have health promoting properties (Bassolino et al., 2013); (Martin et al., 2011), for
67 reviews). It has been shown that the consumption of anthocyanins can lower the risk of cancer,
68 diabetes and cardiovascular diseases (Zafra-Stone et al., 2007); (He and Giusti, 2010); (Tsuda, 2012);
69 (Butelli et al., 2008). To be able to breed for fruits and vegetables that are rich in anthocyanins, it is
70 important to understand both their biosynthesis and functions in plants. By expressing two
71 transcription factor genes, *Rosea1* (*ROS1*) and *Delila* (*DEL*), isolated from *Antirrhinum majus* flowers,
72 under control of the tomato *E8* promoter, which is expressed during fruit ripening, tomato plants were
73 engineered that carry purple fruits (Butelli et al. 2008). These purple tomato fruits, that are otherwise
74 isogenic to red fruits, have been essential for defining health claims for anthocyanins (Martin et al.,
75 2011; Martin et al., 2013).

76 *ROS1/DEL* tomato fruits are enriched with anthocyanins which predominantly include
77 delphinidin 3,5-diglycosides and are acylated with hydroxycinnamic acids (Butelli et al., 2008).
78 Overexpression of *ROS1/DEL* transcription factors in tomato led to the induction of expression of a
79 number of genes homologous to known genes from the anthocyanin pathway in *Arabidopsis* and
80 petunia (Butelli et al., 2008). In tomato, the role of some of these genes in anthocyanin biosynthesis
81 has been confirmed using mutants disrupted in the *FLAVONOID 3-HYDROXYLASE* (*F3H*) gene
82 (Maloney et al., 2014) and the *DIHYDROFLAVONOL 4-REDUCTASE* (*DFR*) gene (Goldsbrough et
83 al., 1994). The tomato anthocyanin-specific O-methyltransferase (*SIOMT*) was identified by a
84 transcriptional analysis of a tomato seedling system, in combination with an interfering RNA strategy
85 (Gomez Roldan et al., 2014). A next step in the understanding of anthocyanin biosynthesis in tomato
86 should focus on the dynamic coordination and gene regulation of the anthocyanin pathways in time,
87 and its integration within plant developmental programs.

88 Transcription factors (TF) that regulate anthocyanin biosynthesis have been identified in many
89 plant species (Petroni and Tonelli, 2011). A complex of three TFs (MBW), including an R2R3-Myb type
90 TF, a basic helix-loop-helix type TF (bHLH) and a WD repeat TF (WDR), was shown to control
91 anthocyanin accumulation (Xu et al., 2015) and in some cases other flavonoids, in many plant species,
92 including *Arabidopsis*, maize and petunia (Albert et al., 2014). In tomato, two highly homologous Myb
93 TFs, *ANT1* and *AN2*, have been shown to be involved in the regulation of anthocyanin biosynthesis
94 (Mathews et al., 2003); (Zuluaga et al., 2008). R2R3-Myb proteins, such as *ROS1* and bHLH proteins
95 such as *DEL*, serve as transcriptional activators of anthocyanin biosynthesis (Broun, 2005). In
96 contrast, *CAPRICE* (*CPC*), a R3-type Myb TF, serves as a negative regulator of anthocyanin
97 biosynthesis in *Arabidopsis*. *CPC* inactivates the MBW protein complex by competing with R2R3-MYB
98 binding to a bHLH TF, while being unable to activate transcription (Tominaga et al., 2008). Related
99 Myb and bHLH TF complexes can control other biosynthetic processes, such as glucosinolate
100 biosynthesis (Frerigmann et al., 2014).

101 Interestingly, specific aspects of cellular differentiation such as root hair and trichome
102 differentiation are also regulated by MBW complexes (reviewed in (Broun, 2005); (Xu et al., 2015);
103 (Tominaga-Wada et al., 2013). For example, in *Arabidopsis* an MBW complex including
104 *WEREWOLFE* (*WER*), *GLABRA3* (*GL3*) and *Transparent Testa Glabra* (*TTG*) controls the
105 transcription of *GLABRA2* (*GL2*), a TF, which acts on root and trichome developmental programs

106 (Rerie et al., 1994); (Bernhardt et al., 2005). Recently it was suggested that MBW complexes
107 controlling secondary metabolism may have evolved from similar MBW complexes that regulate more
108 ancient gene networks for differentiation of cell types (Chezem and Clay, 2016).

109 Systematic transcriptomics and metabolomics analysis have been employed to obtain a more
110 holistic view of the regulation of the anthocyanin biosynthetic program. Such studies have been done
111 both on tomato seedlings in which anthocyanin formation is induced by nutrient stress (Roldan et al.,
112 2014) and on purple *ROS1/DEL* fruits (Tohge et al., 2015). In these studies, networks of genes and
113 metabolites were analysed combining data from different tissues and cell types. Genes were identified
114 that encode putative anthocyanin-modifying enzymes and transporters. However, to put anthocyanin
115 biosynthesis in a context beyond biosynthetic genes, one needs to make observations on transcription
116 networks and metabolite profiles which are independent of nutrient stress or developmental changes,
117 and with high resolution in time. To achieve this, a uniform and tightly-controlled system for steering
118 the anthocyanin biosynthetic program is needed.

119 Here, we aimed to study the anthocyanin pathway in tomato and its associated cellular and
120 developmental processes using such a tightly regulated transcription system. We developed, for the
121 first time, an inducible dexamethasone-regulated switch, which can deliver, on-demand, anthocyanin
122 accumulation in different tissues of the tomato cultivar MicroTom. We interrogated the transcriptional
123 and metabolic networks associated with anthocyanin biosynthesis in different vegetative tissues of
124 tomato, including undifferentiated totipotent callus cells. This study revealed new aspects of
125 transcriptional regulation of anthocyanin accumulation in tomato plants, and linked it to epidermal cell
126 fate, in particular in root tissues. We identified several targets of regulation by *ROS1/DEL* TFs
127 including genes involved in epidermal cell fate determination, cuticle formation, auxin biosynthesis and
128 transport as well as several transcription factors. These data can serve as a resource for the
129 identification of genes involved in anthocyanin biosynthesis. As an example, we focussed on specific
130 acyl transferases involved in the addition of hydroxycinnamic acids to the glycoside moieties of tomato
131 anthocyanin *in vivo*. These data provide insight in the processes that may accompany anthocyanin
132 biosynthesis, including physiological and architectural changes in tomato vegetative tissues.

133

134 **RESULTS**

135 **Development of an inducible system for anthocyanin biosynthesis in tomato cv. MicroTom**

136 Previous studies in tomato fruits have shown that substantial induction of anthocyanin biosynthesis
137 can be achieved by ectopically expressing two transcription factors (*ROS1/DEL*) from snapdragon
138 (Butelli et al., 2008); (Tohge et al., 2015). These studies use the fruit specific promoter E8, which is
139 regulated by ethylene and thereby is specifically activated during the breaker stage of fruit ripening.

140 To collect comprehensive information about the gene expression program and metabolic
141 changes that specifically accompany anthocyanin biosynthesis in different tissues and at different time
142 points during plant development, a tomato system was engineered in which *ROS1* and *DEL*
143 expression could be experimentally induced by exogenous application of dexamethasone (DEX). This
144 DEX-inducible system was used as described previously (Aoyama and Chua, 1997). The cDNAs of
145 *ROS1* and *DEL* were both inserted behind synthetic promoters containing repeats of the upstream
146 activating sequence of the yeast *gal4* gene. These promoters were regulated by a DEX regulated
147 chimeric transcription factor GVG, consisting of the DNA-binding domain of the yeast transcription
148 factor GAL4, the transactivation domain of the herpes viral protein VP16, and the receptor domain of
149 the rat glucocorticoid receptor (GR). Expression of the GVG was driven by the constitutive *Arabidopsis*
150 *UBIQUITIN10* (*UBQ10*) promoter (Dijken et al., 2004).

151 The three cassettes (*GAL4-ROS1*; *GAL4-DEL* and *UBQ10-GVG*) were combined on a single
152 plasmid as part of the same T-DNA (Fig. 1A). Transformation of this construct to *S. lycopersicum*
153 Microtom yielded a number of transgenic calli, which were analyzed for presence of the transgenes by
154 exposing them to DEX, upon which some of them turn purple (Fig. 1B). Some positive calli were
155 maintained as undefined tissue, while others were regenerated into independent transgenic lines,
156 *ROS1/DEL* lines 4, 8 and 11. Application of DEX to these plants, either by direct contact or by
157 inclusion in the water supply to the soil, resulted in the formation of a purple colour in most of tested
158 tissues (Fig. 1). This included vegetative tissues such as roots, stems and leaves (Fig. 1, C-D). In
159 contrast, in none of the lines, formation of purple colour was observed in flowers or fruits upon
160 application of DEX, even not when DEX was directly applied to these tissues.

161 It has been shown before that upon high accumulation of anthocyanins, anthocyanin vacuolar
162 inclusions (AVIs) are formed inside the cell vacuoles in different plant species (Grotewold, 2006);
163 (Chanoca et al., 2015). The accumulation of such AVIs were also observed here in tomato leaf
164 epidermal cells when anthocyanin formation was induced by DEX (Supplemental Fig. S1A).

165 ***ROS1* and *DEL* induced metabolites in tomato seedlings**

166 When *ROS1/DEL* were expressed in the leaves of *Nicotiana*, a single anthocyanin and a
167 range of non-flavonoid phenolic compounds (e.g. polyamine and nor-nicotine conjugates) were
168 produced (Outchkourov et al., 2014), while in tomato fruit, *ROS1/DEL* expression lead to production
169 of a set of complex anthocyanins and flavonoids (Butelli et al., 2008; Tohge et al., 2015). This
170 suggests that the identity of *ROS1/DEL* regulated metabolites depends on the species or tissue, but at
171 present there are no data available of the consequence of *ROS1/DEL* expression in tomato vegetative
172 tissues. To test this, *ROS1/DEL* were induced in leaf and root tissue from *ROS1/DEL* line 4, and an
173 untargeted metabolite analysis was performed. Seedlings were incubated with or without the addition
174 of DEX for 24 hours, 5d and 14d, then extracted with methanol and analysed by liquid
175 chromatography - photodiode array – mass spectrometry (LC-PDA-MS) (Fig. 2, A-C and Supplemental
176 Fig. S1, B-C). A rapid induction of anthocyanins (absorbing at 520 nm) was observed within less than
177 24 hours after DEX application, in both roots and aerial parts of the seedlings (Fig. 2, A-C and
178 Supplemental Fig. S1, B-C). MS analysis allowed the identification of seven anthocyanins (Fig. 2C,
179 Supplemental Table S1), all of which had been previously identified in tomato hypocotyls and
180 *ROS1/DEL* fruit (Roldan et al., 2014; Tohge et al., 2015). Both tissues contained the same
181 anthocyanins, but at different ratios and with different kinetics. In roots, maximum induction of
182 anthocyanins was reached within 24 hours, whereas in the aerial parts of the seedlings this was
183

184 reached only after 5 days. In the absence of DEX, roots did not contain detectable anthocyanins, while
185 only minor amounts were found in the aerial parts of the seedlings.

186 To identify other metabolites regulated by *ROS1/DEL* induction, an untargeted analysis of the
187 LC–MS data was performed. In both tissues, the anthocyanins and a number of related flavonoids
188 were found to be the dominant compounds, while other compound categories were much less
189 obviously represented. In root tissue, 63 metabolites were found to be more than two-fold upregulated
190 by DEX treatment (Supplemental Table S1A). In addition to the seven anthocyanins, seven flavonols
191 were also found to be induced in time by DEX. Furthermore, four dexamethasone-derived metabolites
192 were observed as well, in addition to dexamethasone itself. Thirty metabolites were found to be more
193 than two-fold downregulated by dexamethasone treatment. For most of those, no identity could be
194 assigned, but some ferulic acid conjugates (e.g. feruloyl-quinic acid, feruloyl-tyramine and feruloyl
195 octopamine) were observed. In shoots, 69 metabolites were consistently found to be more than two-
196 fold upregulated by dexamethasone treatment. Most identifiable and major compounds (anthocyanins,
197 flavonols, DEX metabolites) correspond to those observed in roots (Fig. 2, Supplemental Table S1B
198 and Supplemental Fig. S1, D-G). DEX itself was not visible in shoot tissue, suggesting that it can only
199 reach the aerial parts after conjugation. Seventeen metabolites were significantly downregulated by
200 dexamethasone treatment, none of which could be identified.

201 A few tissue-specific changes were observed. For example, the root feruloyl conjugates found
202 to be downregulated by DEX were not detectable in shoot tissue, even in the control samples. In
203 shoots, chlorogenic acid increased upon dexamethasone treatment after 24h, and had increased
204 further after 5 days and 14 days. In root tissue, an increase was only observed after 24h, while
205 chlorogenic acid levels did not differ significantly from the control after 5 or 14 days (Supplemental Fig.
206 S1, D-G). Thus, *ROS1/DEL* expression induced predominantly anthocyanin in tomato leaf and root
207 tissue, in addition to a number of flavonoids, most of which were known to be induced in tomato fruit.
208 In contrast to *Nicotiana*, no major changes in non-flavonoid metabolites could be observed in tomato
209 root and shoot.

210 **Transcriptome analysis in callus and roots**

211 To obtain a detailed understanding of *ROS1/DEL* function in regulating secondary
212 metabolism, we identified genes that are controlled by these TFs on a genome-wide scale in both
213 undifferentiated and differentiated tissue. Studying callus tissue, consisting of basically uniform, non-
214 differentiated cells, has the advantage that developmental programs will not influence the
215 transcriptional response to *ROS1/DEL* expression. On the other hand, root tissue is highly
216 differentiated and can respond rapidly to developmental cues, which will allow to address the
217 interaction of *ROS1/DEL* controlled secondary metabolism with developmental processes. Therefore,
218 transcriptional changes upon *ROS1/DEL* activation were studied in roots of *ROS1/DEL* line 4 and of
219 three callus cultures from independent primary transformation events. Time points were selected
220 based on the presence of the anthocyanin biosynthetic proteins, anthocyanin synthase (SIANS) and
221 dihydroflavanol 4-reductase (SIDFR), which have both previously been shown to be induced by *ROS1*
222 and *DEL* (Butelli et al., 2008). Antisera were developed that recognize recombinant SIANS or SIDFR
223 proteins and these were used to monitor expression of both proteins by western blot. SIANS was
224 detectable as early as 3h after induction and was increased significantly after 24h in both callus and
225 roots (Supplemental Fig. S2). The DFR protein was clearly detectable after 24h. Therefore, samples
226 for transcriptome analysis were taken after 3h and 24h.

227 *In vitro*-grown callus, deriving from three different primary transformants (T0) and seedlings of
228 line 4 (T2 generation) were transferred to fresh media with and without DEX and samples were
229 collected at 3 and 24h post induction. RNA was extracted and cDNA was analysed by Illumina
230 sequencing. Reads were mapped onto tomato gene models to which the *ROS1* and *DEL* cDNA
231 sequences were added, and gene expression data were calculated. In total, expression of 5295 genes
232 significantly changed more than two-fold ($n=3$; $FDR < 0.05$) for at least one of the time points or
233 tissues, relative to untreated materials. Genes that were affected by *ROS1* and *DEL* induction across
234 all tissues and time points formed only a small subset of these genes, as can be observed in the Venn
235 diagrams in Fig. 3A. From a total of 5295 differentially-regulated genes, 220 were consistently

236 upregulated and 205 were consistently down regulated in both tissues, callus and roots, and at both
237 time points. This set of overlapping genes was used as the core of 425 genes affected by *ROS1* and
238 *DEL* (Supplemental Table S2).

239 To obtain an overview of the functional implications of transcriptional changes mediated by
240 ROS and DEL induction, gene ontology (GO) annotations for the 425 consistently regulated core
241 genes were analyzed (Fig. 3B). This was done by comparing, for each GO category, its frequency
242 among the 425 core genes to its frequency among all annotated genes in the tomato genome. In this
243 way, GO categories that were overrepresented among the set of up-regulated or among the set of
244 down-regulated genes were obtained. Significantly overrepresented GO categories among the
245 upregulated genes were involved in the biosynthesis of phenylpropanoids, flavonoids and
246 anthocyanins, as well as responses to different types of known anthocyanin-related stresses such as
247 carbohydrate stimuli (Das et al., 2012). These functions obviously are relevant for the well-known role
248 of *ROS1/DEL* in anthocyanin biosynthesis. Interestingly, the upregulated genes were also enriched
249 for GO categories involved in lipid biosynthesis and epidermal cell specification. Among the genes
250 down-regulated by *ROS1/DEL* expression, GO terms involved in cell wall organization, root
251 morphogenesis and the differentiation of trichomes and epidermal cells were overrepresented. It is
252 remarkable that GO categories that are known to function in specific differentiated tissues (e.g. root
253 epidermis, leaf trichomes) were found to be consistently regulated by *ROS1/DEL*. Apparently, genes
254 with these functions are also regulated by *ROS1/DEL* in undifferentiated callus, where they have no
255 clear significance to the tissue.

256

257 **Regulation of pathways leading to anthocyanins by *ROS1* and *DEL* activation**

258 The effect of *ROS1* and *DEL* gene expression on the regulation of individual genes was
259 analysed. Already after 3h of induction, *ROS1/DEL* already strongly activated genes of the
260 anthocyanin pathway, both in callus and in roots (Table 1). In view of the observation that no
261 anthocyanins could yet be detected at these stages, this would indicate that these genes are directly
262 regulated by *ROS1/DEL*, and not by the presence of anthocyanins. Genes involved in converting
263 phenylalanine to polyphenols including anthocyanins mostly overlapped with those identified to be
264 upregulated in *ROS1/DEL* fruits, encoding enzymes and transporters from the pathway leading to
265 anthocyanins, flavonoids and chlorogenic acid (Butelli et al., 2008); (Tohge et al., 2015). Interestingly,
266 several genes from the phenylalanine biosynthetic pathways were also activated after 3 hours by
267 *ROS1/DEL*, including shikimate kinase (*SK1*), a key enzyme of the shikimate pathway towards
268 phenylalanine, and cytosolic pyruvate kinase and acetyl coA carboxylase, involved in malonyl CoA
269 biosynthesis (Table 1 and Fig. 4). Transketolase, an important enzyme in the pentose phosphate
270 pathway, which converts glucose to supply erythrose 4-phosphate (the starting point of the shikimate
271 pathway) was initially down-regulated in roots, while being upregulated after 24h (Table 1). Likely this
272 indicates that the pentose phosphate pathway is not under direct regulation of *ROS1* and *DEL*, but is
273 upregulated in the root when an enhanced supply of carbon into the shikimate pathway is needed.

274 Biosynthetic genes not known to participate in anthocyanin biosynthesis were also found to be
275 regulated by *ROS1/DEL* expression, including for instance, genes important for auxin homeostasis. A
276 number of auxin transporter genes (*PINs* and *LAXs*) were already found to be downregulated 3h after
277 DEX induction (Table S2). Gene homologous to *Auxin-regulated Indole-3-acetic acid-amido*
278 *synthetase*, *GH3.4* (Liao et al., 2015) was up-regulated upon DEX addition (Table S2). *GH3* genes in
279 plants have been shown to regulate auxin homeostasis levels by conjugating the excess of active IAA
280 (indole acetic acid) to an inactive form.

281

282 **Regulation of a transcriptional network involved in epidermal differentiation**

283 Upon upregulation of *ROS1* and *DEL*, a considerable number of other transcription factors
284 were observed to be activated in both callus and roots (Table 1 and Table S2). From the core of 425
285 genes a total of 27 genes were transcription factors, most of which (22) were upregulated. This
286 indicated the possibility that *ROS1/DEL* not only directly activate biosynthetic genes in the anthocyanin
287 pathway but also regulate or at least influence, a more complex transcriptional network. Interestingly,

288 among the *ROS1/DEL*-regulated TF genes, were several that are annotated with the GO-category
289 epidermal cell fate. One of these genes is the tomato *MIXTA-like* TF, which is a key regulator of
290 epidermal cell patterning and cuticle assembly in tomato fruit (Lashbrooke et al., 2015). Also, a
291 homologue of *Glabra2* (*GL2*), known to be involved in root and trichome developmental programs in
292 *Arabidopsis* (Rerie et al., 1994);(Bernhardt et al., 2005), was 6-fold upregulated in callus and 30-folds
293 in roots after DEX induction. Surprisingly, one of the most strongly up-regulated TFs (125 fold in roots)
294 only 3h after DEX induction is homologous to the Arabidopsis root-hair regulator *CPC*.

295 **Confirmation of the activation of root-morphology and auxin-related genes using quantitative** 296 **real time PCR** 297

298 Transcriptome analysis was based on a comparison of tissues from induced and non-induced
299 plants from the same genotype, to avoid noise from genotype-related differences in the data. Gene
300 expression changes relevant for root morphology and for auxin regulation, were validated to confirm
301 their dependence on the expression of *ROS1/DEL*, and not to result from the application of DEX *per*
302 *se*. qPCRs were performed for a subset of genes, comparing *ROS1/DEL* plants (T4 generation) to WT
303 seedlings both of which were treated with DEX. The qPCR results confirmed the up-regulation of
304 *GH3.4* and *GL2* and the downregulation of *PIN6* and *PIN9*, observed from the transcriptomics results
305 in roots treated with DEX for 3h and 24h (Fig. 3, C-D). Furthermore, we observed up-regulation of
306 *GH3.4* and *GL2* in the aerial parts of seedlings incubated with DEX for 3 and 24h (Fig. 3C).

307 **Activation of the tomato *GL2* promoter by *ROS1/DEL* in Nicotiana** 308

309 To confirm that the tomato *GL2* homologue is a possible direct target of *ROS1/DEL*, a reporter
310 transactivation assay was used. The tomato *GL2* promoter was fused to a luciferase reporter gene
311 (pGL2-LUC), which enables the visualization of *GL2* promoter activation. *N. benthamiana* leaves were
312 agro-infiltrated with pGL2-LUC alone, or in combination with 35S:ROS1 and 35S:DEL constructs
313 (Supplemental Fig. S3, A-B). After 3 days post infiltration, the leaves were sprayed with luciferin and
314 incubated for 1 more day, after which luciferase activity was measured. The pGL2-LUC construct
315 alone resulted in very low luminescence (Supplemental Fig. S3, A-B) whereas the luciferase activity
316 was strongly induced by co-infiltration of pGL2-LUC with *ROS1/DEL*, confirming that *ROS1/DEL*
317 control *GL2* expression also in leave tissue.

318 **Tissue specific gene activation by *ROS1/DEL*** 319

320 Besides the genes found to be regulated in both callus and root tissues and at both time
321 points, a number of GO-categories was found to be overrepresented among genes regulated
322 differentially in only one of the tissues (Supplemental Fig. S4A). This analysis was performed in the
323 same way as described above for the set of 425 genes, but this time separately per tissue. Specifically
324 for genes differentially regulated in callus, a set of genes involved in transcriptional regulation was
325 observed. These genes consisted of a set of 18 TFs, from diverse TF families. These TFs are different
326 from those identified to be regulated in all tissues (the core set of genes). Also the GO term
327 "oxidoreductase activity" was found exclusively in callus; This category included genes involved in
328 ethylene biosynthesis, such as five *1-aminocyclopropane-1-carboxylate oxidases* (*ACO*), two of which
329 (including *ACO2*) were up-regulated by *ROS1/DEL* in callus, while three were downregulated.

330 In roots, compared to callus, a larger set of GO categories was found to be overrepresented in
331 genes that were differentially regulated by DEX-induced *ROS1/DEL* expression (Supplemental Fig.
332 S4A and Supplemental Table S3). A number of these categories relate to lipid metabolism, for
333 instance categories lipid transport and lipid localization and lipid metabolic processes. The regulated
334 genes in these categories encode enzymes involved in cuticle polymerization (e.g. *GDSL1/cutin*
335 *deficient 1* which was 94 fold up-regulated in roots) (Girard et al., 2012); (Yeats et al., 2014) and
336 several lipid transfer proteins. Interestingly, two of the highly up-regulated genes identified in both
337 callus and roots correspond to *LACS1* (*long chain acyl-CoA synthase 1*) and the tomato homologue of
338 *CER1*, both of which have been predicted to be involved in cutin monomer synthesis (Lu et al., 2009);
339 (Girard et al., 2012) (Table 1). Thus, the transcriptomics data suggest a positive link between
340 anthocyanins biosynthesis and cuticular wax biosynthesis. Another GO category, antioxidant activity,

341 comprised five peroxidases, 4 of which were strongly downregulated upon *ROS1/DEL* expression in
342 roots. In the GO category, response to biotic stimuli, we found three highly up-regulated genes (from
343 87 to 160 fold), which encode homologues of the birch pollen allergen *Bet v 1* (Munoz et al., 2010),
344 while other genes from the same protein family were downregulated by *ROS1/DEL*.

345 **Functional analysis of the *ROS1* and *DEL* activated genes**

346 For functional analysis of genes regulated by *ROS1* and *DEL*, a Virus Induced Gene
347 Silencing (VIGS) system was used in combination with DEX induction of *ROS1/DEL* in Microtom
348 seedlings. The efficiency of VIGS was tested by silencing the *PHYTOENE DESATURASE (PDS)* gene
349 in parallel to the genes of interest. Silencing of PDS resulted in photo bleaching (Supplemental Fig.
350 S5A), causing white patches and white leaves and is therefore easily detected visually (Velasquez et
351 al., 2009); (Zheng et al., 2010). After 11 days, white patches and white leaves were observed, mainly
352 in the newly formed leaves. After induction, by transferring seedlings to DEX-containing medium the
353 white patches became bright purple (Supplemental Fig. S5A).

354 Among the genes that were highly upregulated by *ROS1/DEL*, were putative anthocyanin
355 acyltransferases (*AAT*), which could potentially contribute to modification of the anthocyanins. Two
356 *AAT* genes, Solyc08g068710, here referred to as *AAT-1*, and Solyc12g088170, referred to as *AAT-2*,
357 were tested for their effect on anthocyanin biosynthesis. While *AAT-1* silencing did not result in any
358 significant changes in anthocyanin content or composition, the effects of *AAT-2* were clearly visible in
359 an LC-MS analysis (Supplemental Fig. S5B). Major tomato anthocyanins, such as petunidin 3-(*trans*-
360 *p*-coumaroyl)-rutinoside-5-glucoside and delphinidin 3-(*trans*-*p*-coumaroyl)-rutinoside-5-glucoside
361 were downregulated by silencing *AAT-2*, while delphinidin 3-rutinoside, lacking an acylgroup, was
362 strongly upregulated. Similarly, some less-abundant quercetin acylconjugates were strongly
363 downregulated upon silencing of *AAT-2* (Supplemental Fig. S5B). These metabolic changes support a
364 role for this gene in acylation of anthocyanins as well as other flavonoids in tomato. The role of *AAT-2*
365 in acylation of anthocyanins was already supported by *in vitro* enzyme activity experiments, and
366 overexpression of the gene in tobacco flowers (Tohge et al., 2015).

367

368 **Physiological and developmental effects of *ROS1/DEL* induction in different tomato tissues**

369 As observed from the RNA sequencing data and the qRT-PCR data, *ROS1/DEL*
370 overexpression upregulates the expression of the tomato *GL2* homologue (Fig. 3C and Table1). In
371 *Arabidopsis*, *GL2* has been reported to promote trichome development and to inhibit both root-hair
372 formation (Ohashi et al., 2002);(Masucci et al., 1996) and stomata formation (Lin and Aoyama, 2012).
373 We therefore hypothesized that *ROS1/DEL* overexpression, through upregulation of a homologue of
374 *GL2*, would have similar effects on tomato. Therefore, several tissues were inspected for
375 morphological perturbation.

376 To address the effect of *ROS1/DEL* overexpression on root morphology, 5d old seedlings of
377 *ROS1/DEL* lines 4, 8 and 11, WT and EV (control) plants were transferred to tilted MS-agar plates with
378 or without DEX. After 4d of growth, the newly-formed parts of the root were studied for root-hair length.
379 The *ROS1/DEL* plants showed purple roots with much shorter root-hairs than plants grown on plates
380 without DEX (Supplemental Fig. S6A). For *ROS1/DEL* line 4 and WT seedlings, root hair length was
381 quantified (n=12), and was observed to be 10-fold reduced upon DEX induction (Fig. 5). Within one
382 root, the intensity of the purple colour of the root appeared to correlate with a reduction in root-hairs
383 (Fig. 5B). No significant change in root-hair length or density occurred when WT tomato plants were
384 placed on DEX (Supplemental Fig. S6B). Also the number of lateral roots was quantified after 12 days
385 on plates with and without DEX. While EV and WT plants did not display a significant difference in the
386 number of lateral roots upon DEX induction, seedlings from *ROS1/DEL* lines 4, 8 and 11 developed
387 significantly more (up to 2-fold) lateral roots on DEX, in comparison to plants transferred to medium
388 without DEX (Fig. 5, C-D).

389 In leaf epidermis tissue, effects of *ROS1/DEL* induction on the morphology could not be
390 observed, apart from the purple-coloured AVIs (see above). Upon prolonged exposure of 6-weeks old
391 WT and *ROS1/DEL* plants to DEX for 5-10d, no changes in the number of trichomes or number of

392 stomata on newly-formed leaves could be observed using microscopy (Supplemental Fig. S5, A-B).
393 Also, no changes in chlorophyll levels were observed by spectral analysis (Supplemental Fig. S5D).
394 Notably, leaf conductance in the DEX-induced *ROS1/DEL* plants was reduced by \pm 25%
395 (Supplemental Fig. S5C). However no consistent differences in stomatal opening could be observed
396 using a binocular microscope, indicating that transpiration rates are potentially lowered in these plants
397 by other mechanisms.

398 Seed germination was strongly affected by *ROS1/DEL* overexpression. While DEX itself
399 hardly affects germination of control seeds, germination of *ROS1/DEL* seeds of lines 4 and 11 was
400 strongly delayed on DEX medium, compared to non-DEX medium (Supplemental Fig. S6C). When
401 seedlings were germinated on non-inducing medium, and then transferred to DEX containing medium
402 after 5d, no growth retardation upon *ROS1* and *DEL* activation was observed.

403 Combined these results strongly indicate that regulation of anthocyanin signalling is linked to
404 various developmental programs, some of which are executed in a tissue specific manner.

DISCUSSION

In this work, we have engineered tomato plants with a DEX-inducible system for anthocyanin biosynthesis, to study the systems biology of a secondary metabolic pathway in tomato. This is the first time that such a system has been used in a crop species such as tomato. The use of DEX-mediated promoter control allows for the precise characterization of responses to regulatory genes, such as transcription factors, and is here used to drive expression of a well-known transcription-factor pair, *ROS1* and *DEL*. In *Arabidopsis*, the DEX promoter system has mainly been deployed to study gene expression programs associated with organ development, e.g. by overexpression of TFs regulating flower formation (Kaufmann et al., 2010) or trichome patterning (Lloyd et al., 1994), and recently, also processes such as secondary cell wall formation (Li et al., 2016). Myb transcription factors such as *ROS1* have hardly been studied before with such tight DEX inducible systems (Morohashi and Grotewold, 2009), probably because these TFs often do not tolerate the presence of C-terminal tags such as the glucocorticoid binding domain. An indirect induction system, using an artificial TF and artificial promoters, such as used here, avoids this limitation, and allows studying the activity of the native TFs. One could exploit such an inducible system to monitor specific responses of plants and plant organs to secondary metabolic pathways.

Expression of *ROS1* and *DEL* in tomato is known to lead to the production of anthocyanins in fruits (Butelli et al., 2008), but was never addressed in root or callus tissues. In particular, purple coloration of tomato root is not known to occur in WT tomato plants. The DEX-inducible system as it was deployed here in tomato led to controlled anthocyanin production in leaves, stems, roots and undifferentiated callus within 24h of induction. It can be used in tissue culture, in whole plants that are grown *in vitro* or in soil. This allows us to monitor gene expression programs and metabolite profiles that are directly controlled by the *ROS1/DEL* TF pair, which will take place in all these tissues and conditions. In addition, one can observe tissue-specific responses at the transcriptional level which provide insights into the interactions between the *ROS1/DEL*-controlled processes, and the local, organ-specific physiological conditions and developmental programs. These interactions define the role of anthocyanins and their master regulators in the physiology and development of the tomato plant.

Notably, the DEX-inducible system used in this study did not result in anthocyanin formation in tomato flower and fruit tissues. Clearly this provides a limitation to the applications of this system in tomato. Likely this observation relates to poor expression of the *GVG* TF from the *UBI10* promoter in these tissues, since direct application of DEX to fruits and flowers also did not result in appreciable coloration. On the other hand, in the absence of DEX, no anthocyanins could be detected in roots, indicating that the regulation of the *UBI10-GVG* system is sufficiently tight to provide a no-expression condition, which is very useful for systems biology approaches.

***ROS1/DEL* control anthocyanin-biosynthetic genes**

At the metabolite level, the response of tomato tissues to *ROS1/DEL* expression is visibly dominated by anthocyanins and related polyphenolic compounds. Although other metabolites were also consistently induced in all analysed tissues, their numbers are limited and less prominent in the metabolic profiles. Similarly, in tomato fruit, metabolite changes controlled by these TFs were found to be confined to anthocyanins and flavonols (Butelli et al., 2008; Tohge et al., 2015). Accordingly, the *ROS1/DEL* induced genes that encode biosynthetic enzymes for anthocyanins and their precursors largely correspond to those observed in these earlier transgenic studies.

Among the identified biosynthetic genes affected were two *AAT*-encoding genes that could putatively mediate the acylation of anthocyanins. The role of these genes was further explored using a VIGS approach in combination with DEX-induced anthocyanin biosynthesis. Tomato anthocyanins are derived from delphinidin 3-rutinoside, which is modified by methylation on the 3' and 4' position, glucosylated at the 5 position and acylated on the rhamnose (Butelli et al., 2008); Gomez (Roldan et al., 2014). Silencing the expression of one of the putative *AATs* lead to the accumulation of delphinidin 3-rutinoside in tomato leaves, demonstrating the role of this gene in anthocyanin acylation in tomato. Modifications such as methylation and 5-glucosylation apparently depend on rhamnose acylation,

458 since no anthocyanins lacking acyl groups but carrying methyl groups were observed. Also, only small
459 amounts of delphinidin 3-rutinoside-5-glucoside could be observed upon silencing of *AAT-2*. Recently,
460 it was shown that the *SIFdAT1* gene, which corresponds to *AAT-2*, mediates acylation of cyanidin
461 rutinoside in *N. tabacum* flowers (Tohge et al., 2015). The observed dependence of anthocyanin
462 methylation and, to some extent, 5-glucosylation, on acylation is similar to the situation in *Petunia*,
463 where the *gf* mutant, which localizes in an acyltransferase gene, produces anthocyanins that lack acyl-
464 groups, 5-glucosides and methyl groups (Jonsson et al., 1984). Thus, the *AAT-2 / SIFdAT1* is not only
465 required for acylation of anthocyanins, but it is also necessary for their 5-glucosylation and O-
466 methylation.

467 Interestingly, several tissue specific changes in gene expression were observed that can be
468 related to anthocyanin biosynthesis and function. For example, a number of genes of the *Bet v 1*
469 family were observed to be highly regulated by *ROS1/DEL* overexpression only in roots. The *Bet v 1*
470 protein family encodes small lipocalin-like proteins with a hydrophobic core, which may contain
471 polyphenolic compounds such as quercetin (Roth-Walter et al., 2014). A function of these proteins in
472 anthocyanin accumulation was previously suggested from work in strawberry, where down-regulation
473 of *Fra a1*, a *BetV1* homolog, led to colourless fruits (Munoz et al., 2010).

474 A set of genes encoding peroxidases was found to be strongly downregulated only in roots,
475 but not in callus. The role of these peroxidases is likely in controlling damage by scavenging reactive
476 oxygen species (Davletova et al., 2005). Overexpression of *ROS1/DEL* in tomato fruit leads to a
477 higher antioxidant capacity and control of the oxygen burst during fruit ripening (Zhang et al., 2013).
478 Possibly the scavenging of reactive oxygen species by accumulating anthocyanins makes expression
479 of peroxidases redundant, thus leading to their down-regulation. However, it remains unclear why such
480 down-regulation is only observed in roots, and not in callus.

481

482 **Regulation of epidermal programs**

483 The DEX-controlled system for expression of *ROS1/DEL* apparently controls processes
484 beyond anthocyanin biosynthesis. In fruits, effects of *ROS1/DEL* on ripening and glycoalkaloid
485 accumulation have been observed (Tohge et al., 2015, Zhang et al., 2013). In the current work,
486 substantial morphological changes were observed in roots, with regard to architecture and epidermal
487 morphology, and in stomatal conductance. The transcriptomics analysis provides leads for
488 mechanistic explanations of these phenomena. For instance, genes involved in auxin homeostasis
489 and auxin flux, such as *GH3.4*, *PINs* and *LAX* (Liao et al., 2015) were already found to be strongly
490 regulated 3h after DEX induction in root, callus and leaf tissue. Auxin is known to control formation of
491 lateral roots and root hair elongation (Overvoorde et al., 2010); (Maloney et al., 2014). In addition,
492 genes involved in epidermal cell fate regulation are strongly regulated by *ROS1/DEL* expression.
493 Among those is a *MIXTA-like* TF gene, which was shown to regulate the epidermal cell patterning and
494 cuticle assembly in tomato fruit (Lashbrooke et al., 2015). Genes known to act downstream of *MIXTA-*
495 *like* were also observed to be strongly regulated by *ROS1/DEL*, for example genes involved in
496 cuticular wax biosynthesis, such as *CER1* and *GDSL1-cutin deficient 1*, and *GL2*. *GL2* is known in
497 *Arabidopsis* to play a role in root hair patterning (Girard et al., 2012); (Yeats et al., 2014), but its role in
498 tomato has never been addressed. Now that these genes have been identified as putative actors on
499 architecture and epithelial morphology in roots, more detailed functional studies are needed to
500 elucidate their exact role in those processes.

501 Our results suggest that *ROS1/DEL* orchestrates anthocyanin biosynthesis by integrating and
502 regulating a network of transcription factors, metabolic enzymes and transporters, growth, patterning,
503 and hormonal pathways in tomato. Moreover, the presented data indicate that anthocyanin-regulating
504 TFs like *ROS1* and *DEL* can be linked to a more broader set of stress responses than solely
505 anthocyanin accumulation. As with anthocyanins, the architectural changes in roots can also be
506 related to stress due to nutrient availability and drought (Lopez-Bucio et al., 2003);(Kovinich et al.,
507 2015). Also effects on cuticle-related gene expression and stomatal conductance could similarly be
508 linked to protection against stress. One could interpret these results to hypothesize that MYB/bHLH
509 transcription factor complexes share a number of programs that allow the adaptation of the plant to
510 environmental changes. Thus, regulation of secondary metabolites such as anthocyanins appears as

511 an integral part of the plant's adaptive repertoire, which also includes developmental and physiological
512 programs. By using an inducible system for expression of such TF complexes, one can study these
513 programs and their phenotypic consequences in different tissues, and provide novel leads for
514 mechanisms which can be recruited by a plant for its survival and adaptation.
515

516 **CONCLUSIONS**

517 Anthocyanins are important in plants for protecting them against stress, and they are also important
518 antioxidants in the human diet. Here a fully inducible system to make anthocyanins on demand is
519 presented. With this we show that anthocyanin biosynthesis is integrated with changes in the
520 architecture of the root.

521 MATERIALS AND METHODS

522 Plant Growth conditions

523 Tomato plants (*Solanum lycopersicum*) cultivars MicroTom and transgenic *ROS1/DEL* plants were
524 grown in the greenhouse at ambient temperatures (>20°C) under natural light supplemented with
525 artificial sodium lights, following a 16-h-light/8-h-dark cycle. Activation of *ROS1/DEL* seedlings by
526 dexamethasone was done by placing seedlings on agar containing 10 mg/L dexamethasone.
527 Dexamethasone was dissolved in ethanol at 10 mg/ml and diluted 1000x in the agar. As a negative
528 control the same volume of ethanol was used. To increase *ROS1/DEL* activation, 3 mg/ml DEX was
529 dripped with 10 µL drops on top of the agar near the plants. Induction experiments were done in round
530 (base diameter 9 cm top 10.5 cm x 14 cm height) sterile plastic plant containers with a breathing strip.
531 For the VIGS experiments, 33d old plants were used with a maximum of 3 plants per pot
532 supplemented with 200 mg/L cefotaxim and 50 mg/L vancomycin in the medium. Root development
533 studies were done on large 24.5 x 24.5 cm plates with 0.6 cm of 1.3 % Duchefa daisin agar and 0.5x
534 Duchefa MS medium. Five days after germination seedlings were transferred to plates with or without
535 DEX. Only seedlings with intact roots were used. Plates were tilted between 45° and 60° and grown at
536 25°C.

537

538 Generation of inducible *ROS1/DEL* transgenic Plants

539 The DEX inducible system pTA7002 (Dijken et al., 2004) was modified by placing the genes *ROSEA1*
540 and *DELILA* from *A. majus* under the control of a DEX activated fusion protein constitutively expressed
541 by the *UBIQUITIN10* promoter. Coding sequence of *ROS1* and *DEL* from (Outchkourov et al., 2014)
542 were amplified using the primers: XhoI_ROS, ROS_SpeI and XhoI_Del, Del_SpeI (TableS4) and
543 ligated into the pTA7002 (UBQ10) (Dijken et al., 2004) vector digested with XhoI and SpeI restriction
544 enzymes to generate pTA7002(UBQ10)-*ROS1* and pTA7002(UBQ10)-*DEL* constructs. Next the
545 pTA7002(UBQ10)-*DEL* vector was modified to contain an extra multiple cloning site
546 (pTA7002(UBQ10)*DEL*-MSC). Briefly pTA7002(UBQ10)-*DEL* was amplified by PCR using
547 oligonucleotides: AsiSI_FW and MauBI_Rev (TableS4). The obtained PCR fragment was ligated into
548 pTA7002(UBQ10)-*DEL* pre-digested with the same enzymes to generate pTA7002(UBQ10)*DEL*-MSC.
549 A new PCR was conducted using the oligonucleotides MauBI_B_FW and ApaI_FW using
550 pTA7002(UBQ10)-*ROS1* as a template and the obtained PCR fragment was ligated in
551 pTA7002(UBQ10)*DEL*-MSC digested with ApaI and MauBI to generate pTA7002(UBQ10) *ROS1/DEL*.
552 The resulting vectors (pTA7002(UBQ10) *ROS1/DEL* and pTA7002) were transformed into
553 *Agrobacterium tumefaciens* strain AGL0 using electroporation and transformed to MicroTom wild-type
554 plants as described before (Karlova et al., 2011; Bemer et al., 2012). Primary (transgenic) callus was
555 obtained during the plant transformation procedure and was maintained on MS medium supplemented
556 with 1.0 mg/l 2,4-dichlorophenoxyacetic acid and 0.1 mg/l kinetin. *ROS1/DEL* positive callus was
557 selected by transferring part of the callus to DEX-containing medium and screening for formation of
558 purple colour after 48h. Seed from T2 to T4 generations, self-pollinated transgenic plants were used
559 for all experiments, including WT segregants from the same population. Seeds were sterilized in 1%
560 bleach for 20 minutes and washed 2 times for 5 minutes in sterile water, dried on sterile filter paper for
561 10 minutes and sowed on 0.8% Duchefa Daisin agar containing 2.2 g/L Duchefa MS with vitamins. 25
562 seeds were used per sterile plastic rectangular container, Duchefa (base: 12 cm x 6.5 cm: top 8 cm x
563 14 cm: height: 7 cm) with a breathing strip in the lid. Containers with seeds were placed at 4°C
564 overnight and grown for 5-9d at 25°C at 16h light/ 8h dark.

565

566 Generation of the constructs

567 Construction of pTRV2 plasmids for virus induced gene silencing

568 Fragments for VIGS were obtained from a frozen sample of purple tomato fruit (Butelli et al., 2008),
569 which was used as a source of RNA. mRNA extraction was performed using the QIAGEN RNeasy®
570 kit. cDNA was synthesized with the Iscript cDNA synthesis kit (BioRad). VIGS fragments were
571 designed by using the VIGS tool from www.solgenomics.com. PCR fragments were obtained with

572 Phusion DNA polymerase (ThermoFisher). AAT VIGS fragments were amplified using primers AAT-
573 2VIGSFw (300bp fragment) and AAT-2VIGSRev, AAT-1Fw and AAT-1Rev. The PDS-VIGS fragment
574 was described previously (Romero et al., 2011). PCR products sizes were confirmed on 1% agarose
575 and excised from gel. The PCR products and pTRV2 vector were digested with *EcoRI* and *XhoI*
576 (NewEngland). Digested PCR products were purified from the gel. pTRV2 and VIGS fragments were
577 ligated with T4 ligase for 3h at room temperature. The full length ORF of AAT-2 was obtained from
578 genomic DNA with the primers AAT-2ORFFw and AAT-2ORFRev. PCR products were gel purified
579 and TOPO cloned into the pCR8/GW/TOPO-TA vector (Invitrogen). After sequence verification the
580 ATT fragment was transferred by GATEWAY recombination to pK7WG2 to create p35S-AAT. The
581 plasmids obtained were then introduced into *Agrobacterium tumefaciens* AGL0 as described before
582 (Outchkourov et al., 2014). All the constructs were verified by sequencing (EZ-seq Macrogen). AGL0
583 harboring an empty pBINPLUS (pBIN) plasmid (Van Engelen et al., 1995) was used as a negative
584 control.

585 **Constructs used for transactivation assay**

586 The *GL2* promoter (pGL2, 1938bp) was amplified from tomato genomic DNA using the primers
587 Gl2promoterFw and Gl2promoterRev (Table S4). The fragment was A-tailed and inserted into the
588 pCR8/GW/TOPO-TA vector (Invitrogen). The sequence was verified and pGL2 was recombined into
589 pGKGWG (containing the GFP reporter gene) and pGreen-LUC (containing the luciferase reporter
590 gene, kindly provided by Dr. Franziska Turck) vectors (Adrian et al., 2010). Plasmids were
591 transformed into *A. tumefaciens* strain AGL0 for plant infiltration.
592

593 **Virus induced gene silencing of *in vitro* tomato seedlings**

594 VIGS was based on the method described before (Gomez Roldan et al., 2014). Seedlings (15 per
595 container) were raised in a container on 0.5xMS agar. The pTRV1, pTRV2, pTRV2-AAT1 and pTRV2-
596 AAT2 vectors in *A. tumefaciens* were grown at 28 °C with shaking in LB medium containing 50 µg/ml
597 kanamycin and 25 µg/ml rifampicin. After 24 h, culture aliquots were transferred to 1.6 mL YEB
598 medium (0.5% beef extract, 0.1% yeast extract, 0.5% peptone, 0.5% sucrose, 2 mM MgSO₄, 20 µM
599 acetosyringone, 10 mM MES, pH 5.6) plus antibiotics, and grown for 3 hrs. After this, the cells were
600 washed twice in 10 mM MgCl₂, 100 µM acetosyringone, and resuspended in co-cultivation medium
601 (0.25 x MS with vitamins pH 6, 0.1% sucrose, 100µM acetosyringone, 0.005% Silwet L-77), and
602 painted onto leaves of 9d old seedlings (T2 generation). After inoculation with *Agrobacterium*,
603 seedlings were kept at 21°C and allowed to recover and grow for 24 days before DEX induction.
604 Activation of *ROS1/DEL* by dexamethasone was done by placing seedlings on agar containing 10
605 mg/L dexamethasone for 3d, after which the seedlings were harvested for analysis.

606 **Trans-activation assays**

607 *Agrobacterium* clones were grown for 24 hours at 28°C in LB medium (10g/L tryptone, 5g/L Yeast
608 extract, 10g/L NaCl) with antibiotics (kanamycin 50µg/ml or spectinomycin 100µg/ml and rifampicin
609 25µg/ml). The OD of the cultures was measured at 600nm and the bacteria were re-suspended in
610 infiltration media (10mM MES buffer, 10mM MgCL₂, 100µm acetosyringone) to an OD of 0.5. After 3h
611 incubation with rotation, leaves of 4-5 weeks old *Nicotiana benthamiana* plants were infiltrated as
612 described before (Outchkourov et al., 2014). After 3 days Agro-infiltrated leaves were sprayed with
613 luciferin (1mM) to inactivate accumulated luciferase. Next day the leaves were again sprayed with
614 luciferin, and 5 minutes after the treatment the leaves were cut from the plant and measured with a
615 cooled CCD camera. Leaves were places on a plastic tray in a box coated with aluminium foil to
616 reduce noise in the pictures caused by cosmic rays. Measurements were made for 5 or 10 minutes.
617 Emission of luminescence has a maximum at 560nm therefore a filter in the camera was used to block
618 most other wavelengths. Analysis of the pictures was performed with ImageJ software. The measured
619 intensity is proportional to the amount of luciferase produced. The intensity of selected areas was
620 measured and values were processed using IPM SPSS Statistics 22.
621

622 **Generation of anti ANS antibody**

623 ORFs of tomato *DFR* and *ANS* genes were PCR-amplified from a total cDNA isolated from purple
624 tomato fruits (Butelli et al., 2008) using the oligonucleotides: tDFR_Fw, tDFR_Rev and tANS_Fw,
625 tANS_Rev. The obtained PCR fragments were gel purified, digested with *EcoRI*-*BglIII* (for *DFR*) and
626 *EcoRI*-*Sall* (for *ANS*) restriction enzymes and ligated into the pACYCDuet-1 vector (Novagen). The
627 newly prepared constructs were sequence verified and immobilized into *E.coli* BL21DE3 cells.
628 Bacterial cultures at an optical density 600 nm of 0.8, were induced with 0.1 mM isopropyl β -D-1-
629 thiogalactopyranoside (IPTG) and incubated overnight at 18°C. Soluble protein was extracted and His-
630 tagged proteins were purified on a Ni-NTA column (Qiagen). Subsequently, fractions containing tDFR
631 and tANS4 protein were further purified over a Superdex 75 (GE Healthcare Life Sciences) 10/30
632 column in 100 mM Tris-HCL pH8 buffer. Protein purity of >95% as visible using SDS-PAGE was used
633 for rabbit immunization at Eurogentec. Western blot analysis was done as described before
634 (Outchkourov et al., 2014). Primary antibodies were diluted 1:1000 and secondary anti-Rabbit IgG
635 (whole molecule)–Alkaline Phosphatase antibody produced in goat (SigmaAldrich A3687) was diluted
636 1:6000. After washing, signals from the blots were developed using substrate tablet BCIP®/NBT from
637 SigmaAldrich.

638 **LC-PDA-MS analysis**

639 Samples of three biological replicates were used for analysis. Semi-polar compounds were extracted
640 and analysed as described in Moco et al. (Moco et al., 2006). Tissues were snap-frozen, and
641 subsequently ground to a fine powder using mortar and pestle. The powder derived from the tomato
642 tissues was weighed exactly (90 - 110 mg dry weight), and was extracted using 10 volumes of 70%
643 methanol solution acidified with 1% v/v formic acid. Samples were sonicated and filtered through a
644 0.45 μ m filter before LC-MS analysis.

645 Separation was achieved using a Luna C18 (2) pre-column (2.0 x 4 mm and an analytical column (2.0
646 x 150 mm, 100 Å, particle size 3 μ m), both from Phenomenex (Torrance, CA, USA). Samples (5 μ l)
647 were injected and eluted using formic acid/water (1:1000 v/v; eluent A) and formic acid/acetonitrile
648 (1:1000 v/v; eluent B) as elution solvents. The flow rate was set at 0.190 mL min⁻¹ with the following
649 linear gradient elution program: 5% B to 35% B over 45 min, with washing for 15 min to equilibrate
650 before the next injection. The column temperature was maintained at 40°C.

651 UV absorbance analysis was performed with a Waters 2996 photodiode array detector (range from
652 240 to 600 nm) and metabolite masses were detected using a LTQ Orbitrap XL hybrid MS system
653 (Waters) operating in positive electrospray ionization mode heated at 300°C with a source voltage of
654 4.5 kV for full-scan LC-MS in the m/z range 100–1500.

655 Acquisition and visualization of the LC-FTMS data were performed using Xcalibur software. The
656 MetAlign software package (www.metAlign.nl) (Lommen, 2009) was used for baseline correction,
657 noise estimation, and spectral alignment. Aligned masses were directly used for further analysis.
658 Comparison and visualization of the main features of the LC-MS data were performed by
659 loading the data matrix into GeneMaths XT 1.6 software (www.applied-maths.com). Metabolite
660 intensities were normalized using log₂ transformation and standardized using range scaling
661 (autoscaling normalization).

662 **RNA-sequencing and data analysis**

664 Primary callus from three independent transformation events (T0 generation) was grown *in vitro* in MS
665 medium supplemented with 1.0 mg/L 2,4-dichlorophenoxyacetic acid (2,4-D) and 0.1 mg/l kinetin.
666 From line ROS1/DEL-04 (T2 generation), four week old seedlings were grown in ½ MS medium, both
667 with 8% agar. Both calli and seedlings were placed on new medium with or without 10 mg/L
668 dexamethasone. Dexamethasone was dissolved in ethanol at 10 mg/ml and diluted 1000x in the agar.
669 As a negative control the same volume of ethanol was used. Triplicates of each induction timepoint –
670 DEX, 3h+DEX and 24h+DEX of both tissues were taken for analysis giving in total 18 samples. Total
671 RNA was extracted from 50 mg ground tissues using the RNeasy Plant Mini Kit from Qiagen according
672 to the manufacturer's instructions. Purified poly(A) RNA was used to produce libraries using a
673 TrueSeq RNA library Prep Kit (Illumina) following the manufacturer's instructions. Pooled libraries
674 were sequenced on an Illumina HiSeq 2000 by WUR-Applied Bioinformatics (The Netherlands).

675 Differential expression was analysed by CLCBIO software, using tomato ITAG2.4 gene models
676 (Tomato Genome, 2012).

677 GO term analysis was performed using the tool available at
678 http://bioinfo.bti.cornell.edu/tool/GO/GO_enrich.html (Boyle et al., 2004). This determines whether any
679 GO terms annotated to a specified list of genes occur at a frequency greater than that would be
680 expected by chance. It calculates a P-value using the hypergeometric distribution followed by
681 Benjamin-Hochberg multiple testing correction, applying a False Discovery Rate cut-off of 0.1.

682

683 **Gene expression analysis by quantitative PCR.**

684 Total RNA was extracted using the RNeasy Plant Mini Kit from Qiagen. cDNA synthesis, and real-
685 time quantitative PCR (qPCR) were performed as described before (Karlova et al., 2013). The primers
686 used for qPCR are listed in Table S4.

687

688 **Microscopy**

689 Micro-Tom wild type and *ROS1/DEL* 7d old seedlings were transferred to plates (base:11cm,
690 high:11cm) with or without DEX. Seedlings were placed \pm 2cm from the top of the plate in order to
691 allow the roots to grow downwards: root length was marked. Plates were placed in an angle of 60°
692 (16h light, 25°C). Microscopy was performed 3d after transferring the seedlings to the plates. Two
693 pictures were made of five roots per treatment. Close-up root pictures to show root hair development
694 were also made by placing the camera on a ZEISS stemi SV11 binocular by means of an adapter.
695 From each picture the length of 10 root hairs was measured using ImageJ. In total, 20 root hairs per
696 root and 100 root hairs per treatment were measured.

697

698 **Scanning electron microscopy (SEM)**

699 Small pieces of Micro-Tom Wild type and *ROS1/DEL* leaves were attached on a brass Leica sample
700 holder with carbon glue (Leit-C, Neubauer Chemikalien, Germany). The holder was fixed onto the
701 cryo-sample loading system (VCT 100, Leica, Vienna, Austria) and simultaneously frozen in liquid
702 nitrogen. The frozen holder was transferred to the cryo-preparation system (MED 020/VCT 100, Leica,
703 Vienna, Austria) onto the sample stage at -92 °C. For removal of frost contamination on the sample
704 surface the samples were freeze dried for 5 min at -92°C and 1.3x10⁻⁶ mbar. After sputter coating with
705 a layer of 20 nm tungsten at the same temperature the sample holder was transferred into the field
706 emission scanning electron microscope (Magellan 400, FEI, Eindhoven, The Netherlands) onto the
707 sample stage at -120°C. The analysis was performed with SE detection at 2kV and 6.3pA. SEM
708 pictures were taken at a magnitude of 250x, and trichomes, hairs and stomata were counted on
709 squares of 500x500µm.

710

711 **Measurement of chlorophyll content with Pigment Analyzer**

712 For non-destructive measurements of total chlorophyll levels, a CP Pigment Analyzer PA1101 (Control
713 in Applied Physiology, Germany) was used according to the manufacturer's instructions.

714

715 **Measurement of stomatal conductance**

716 Stomatal conductance (mmol H₂O m⁻² s⁻¹) was measured on the abaxial side of the leaf, using a
717 Decagon leaf porometer SC-1 (Decagon devices, Pullmann WA, USA).

718

719 **Pictures**

720 Photos were made with a CANON Powershot G12.

721 **Statistical analyses**

722 Statistical analyses were performed using IBM SPSS Statistics 23. For root hair analysis an ANOVA
723 was performed with genotype and DEX treatment in a model. The natural logarithm of the root hair
724 length was calculated to obtain a normal distribution and values were used in the ANOVA (ref) and
725 LSD test. For the luciferase assay background values were subtracted and log values were calculated

726 from remaining luminescence values to achieve a normal distribution. Values were used for a LSD
727 test.
728
729

730 **SUPPLEMENTAL MATERIAL**

731 **Figure S1.** Metabolite analysis of *ROS1/DEL* activated tomato plants.

732 **Figure S2.** Induction of ANS and DFR proteins upon DEX induction.

733 **Figure S3.** Direct activation of *GL2* by *ROS1/DEL* and pleiotropic effects of anthocyanin induction.

734 **Figure S4.** Functional categories of genes significantly regulated by *ROS1/DEL* in a tissue specific
735 manner.

736 **Figure S5.** Virus induced gene silencing of anthocyanin acyltransferase.

737 **Figure S6.** Phenotypic effects of anthocyanin induction in root tissue.

738 **Figure S7.** Phenotypic effects of anthocyanin induction in leaf tissue.

739

740 **Table S1.** Metabolite analysis of roots and shoots of *ROS1/DEL* activated tomato plants.

741

742 **Table S2.** Gene expression profiles after DEX activation of *ROS1/DEL* TFs.

743 **Table S3.** GO categories only in roots. Functional categories of the UP- and Down-regulated tissue
744 specific genes by *ROS1/DEL*

745 **Table S4.** Oligonucleotides used in this study.

746

747 **ACKNOWLEDGEMENTS**

748 The authors have no conflict of interest. The authors would like to acknowledge, Bert Schipper for LC-
749 MS measurements. The authors thank Prof. Cathie Martin for E8:*ROS1/DEL* tomato seeds.

750

751 **ONE SENTENCE SUMMARY**

752

753 A systems biology study reveals that anthocyanin biosynthesis in tomato vegetative tissue is
754 accompanied by changes in the epidermis and architecture of the root.

755

756

757

758 **FIGURES LEGENDS:**

759 **Figure 1. DEX inducible system for anthocyanin accumulation in tomato.** (A) Schematic
760 presentation of the constructs used in the study: Promoter of the *ubiquitin 10* gene from Arabidopsis
761 drives the expression of a chimeric transcription factor consisting of the yeast *GAL4* DNA recognition
762 motive-VP16 activation domain and glucocorticoid binding domain (GR). *ROS1* and *DEL* expression is
763 controlled by a separate cassettes driven by promoter with gal4 binding sites. (B) Representative
764 primary callus before induction and two weeks after induction with DEX. (C) Representative seedlings
765 of *ROS1/DEL* line 4, 5 days after DEX induction. (D) Plants of *ROS1/DEL* line 4 in soil two weeks after
766 induction with DEX.

767 **Figure 2. Metabolite analysis of ROS1/DEL activated tomato plants.** Examples of chromatograms
768 from LC-PDA-MS at 520 nm showing 7 peaks specific for anthocyanins in roots (A) and shoots (B)
769 of tomato seedling, in the absence of DEX, or induced with DEX and sampled after 24 hours, 5 days and
770 14 days. (C) Core structure of the tomato anthocyanins; (D) Identity of the anthocyanins observed in
771 (A).

772 **Figure 3. Gene expression profiles after DEX activation of ROS1/DEL.** (A) Venn diagrams
773 showing the overlap of up- and down-regulated genes ($p < 0.05$, fold 2) in the different tissues and time
774 points. A core of 220 up- and 205 down- regulated genes were identified as tissue and time
775 independent functional targets of *ROS1/DEL*. (B) Functional GO categories of the Up-regulated and
776 Down-regulated genes. Bars represent p-values of GO categories which are significantly
777 overrepresented (left) and underrepresented (right), comparing to all GO-annotated genes on the
778 tomato genome. (C-D) Quantitative RT-PCR confirmation for *GH3.4*, *GL2* (C), *PIN6* and *PIN9* (D)
779 gene expression (n=4 biological replicates; shown are mean values with standard deviations).
780 *ROS1/DEL* line 4 seedlings (T4 generation) and WT seedlings were incubated with DEX for 3h and
781 24h. After that the roots and the shoots were analysed separately.

782 **Figure 4. Genes regulated by ROS1/DEL in the anthocyanin pathway.** Schematic overview of the
783 anthocyanin biosynthetic pathway and the genes changing upon induction with DEX. More intense red
784 colour indicates stronger upregulation.

785 **Figure 5. Phenotypic effects of ROS1/DEL activation on root morphology.** (A) Root hair length of
786 *ROS1/DEL* line 4 plants and WT plants in the presence and absence of DEX. Shown are mean values
787 (n=12) and standard deviation. (B) Sectors with less purple coloration have longer root hairs. (C)
788 Influence of *ROS1/DEL* activation on the number of lateral roots in *ROS1/DEL* line 4. Plants were
789 transferred to media with or without DEX 5 days after germination and scored for lateral roots after 12
790 days of DEX induction. Black dots are placed at the end of each lateral root. (D) Number of lateral
791 roots in the absence and presence of DEX in WT MicroTom, EV control and *ROS1/DEL* lines 4, 8 and
792 11. Shown are mean number of lateral roots (n=7): asterisks indicate significant differences between
793 induced and non-induced seedlings from the same line after 12 days of growth (students t-test: *:
794 $p < 0.05$; **: $p < 0.01$). Error bars represent the standard deviation.

795

796

799 Table 1. Genes regulated upon DEX induction.

Gene number	Gene name	Putative function	Callus 3h	Roots 3h	Callus 24h	Roots 24h	References
Transcription factors putatively involved in the epidermal cell fate							
Solyc09g065100	SlbHLH150	-	63	199	1259	2512	(Sun et al. 2015)
Rosea 1	Rosea 1	anthocyanin biosynthesis	234	316	63	100	(Goodrich et al. 1992)
Delila	Delila	anthocyanin biosynthesis	63	398	40	199	(Schwinn et al. 2006)
Solyc07g052490	MYB-CPC-like	trichome and root hair regulation	20	316	79	158	-
Solyc03g120620	GL2	cuticle regulation	6	39	5	31	(Lashbrooke et al. 2015)
Solyc01g109120	WD40 repeat	-	12	16	25	6	-
Solyc10g055410	SITHM27	anthocyanin biosynthesis	31	6	79	2	(Matus et al. 2009)
Solyc04g072890	WD40 repeat	-	16	10	8	4	-
Solyc03g098200	HDG11 like/GL2 like	-	2.5	6	2.5	10	(Yu et al. 2008)
Solyc02g088190	MIXTA-like	epidermis and cuticle development	2	3	4	8	(Lashbrooke et al. 2015)
Solyc03g097340	TTG1-like	trichome and root hair regulation	5	4	2.5	3	(Galway et al. 1994)
Solyc10g081320	SIMYB69	-	-4	-5	-2	-2	(Stracke et al. 2001)
Solyc09g057710	SlbHLH057	-	4	5	2	2	(Sun, Fan and Ling 2015)
Solyc04g074170	SIMYB39	-	-3	-2.5	-3	-5	-
Solyc05g051550	SIMYB	-	-5	-2.5	-5	-6	-
Solyc09g018500	SlbHLH	-	-20	-10	-20	-32	-
Cutin pathway							
Solyc00g278110	CER1 like	cutin synthesis	29	252	17	199	-
Solyc01g079240	SILACS1	cutin synthesis	100	422	4.3	17	(Girard et al. 2012)
Flavonoid pathway							
Solyc09g091510	CHS2	Chalcone synthase	4	398	125	5011	(Tohge et al. 2015)
Solyc05g052240	CHIL	Chalcone isomerase	20	316	100	631	(Tohge et al. 2015)
Solyc05g010320	CHI	Chalcone isomerase	2.5	3.1	7.9	7.9	(Tohge et al. 2015)
Solyc02g083860	F3H	Flavanone 3-hydroxylase	12	158	16	251	(Tohge et al. 2015)
Solyc11g066580	F3'5'H	Flavonoid-3'-monoxygenase	501	1585	25118	31623	(Tohge et al. 2015)
Solyc02g085020	DFR	Dihydroflavonol 4-reductase	15849	5012	19953	5012	(Butelli et al. 2008)
Solyc08g080040	ANS	Leucoanthocyanidin dioxygenase	126	251	251	251	(Tohge et al. 2015)
Solyc09g082660	AnthOMT	Anthocyanin-O-methyltransferase	501	100	5012	1995	(Gomez Roldan et al. 2014)
Solyc10g083440	A3GT	Anthocyanin-3-O-glucosyltransferase	501	630	398	501	(Butelli et al. 2008)
Solyc09g059170	A3G2"GT	Anthocyanin-3-O-gluc-2"GT	148	631	631	1000	(Tohge et al. 2015)
Solyc12g098590	A5GT	Anthocyanin-5-O-glucosyltransferase	1585	630	25119	10000	(Tohge et al. 2015)
Solyc12g088170	SIFdAT1	Anthocyanin acyltransferase	794	3162	1585	10000	(Tohge et al. 2015)

Solyc08g068700	THT7-1	Acyltransferase	4	2.5	10	2.5	(Von Roepenack et al. 2003)
Solyc03g097500	HCT like	Acyltransferase	-2	-2.5	-2.5	-3	-
Solyc08g078030	HCT like	Acyltransferase	-12	-3	-12	-5	-
Solyc10g078240	C3H	p-coumarate 3-hydroxylase	5	4	4	2.5	(Butelli et al. 2008)
Solyc02g081340	GST	Glutathione-S-transferase	1585	10000	2511	10000	(Butelli et al. 2008)
Solyc10g084960	GST	Glutathione-S-transferase	10	10	6	5	-
Solyc07g056510	GST	Glutathione-S-transferase	6	8	3	3	-
Solyc06g009020	GST	Glutathione-S-transferase	4	5	3	2.5	-
Solyc03g025190	FFT	Flower flavonoid transporter/ putative anthocyanin permease	316	10000	2000	50119	(Mathews et al., 2003)
Pentose phosphate pathway							
Solyc10g018300	Transketolase	Transketolase	-2.5	-4	2	2.5	-
Solyc09g008840	Pyruvate kinase	Pyruvate kinase	3.4	2.5	4	2.6	-
Solyc12g056940	Acetyl-CoA carboxylase	Acetyl-CoA carboxylase	17	12	12	9	-
Shikimate pathway							
Solyc04g051860	SK1	Shikimate kinase	4	4	2.5	2	(Schmid et al., 1992)
Phenylpropanoid pathway							
Solyc02g086770	CCR	Cinnamoyl CoA reductase	40	32	20	10	(Tohge et al., 2015)
Solyc08g005120	CCR	Cinnamoyl CoA reductase	4	8	5	5	-
Solyc03g036480	PAL	Phenylalanine ammonia lyase	6	8	5	5	-
Solyc03g036470	PAL	Phenylalanine ammonia lyase	6	8	6	4	-
Solyc05g056170	PAL6	Phenylalanine ammonia lyase	5	3	10	3	(Tohge et al., 2015)
Solyc09g007910	PAL3	Phenylalanine ammonia lyase	10	2	5	2	(Tohge et al., 2015)
Solyc03g042560	PAL	Phenylalanine ammonia lyase	5	6	6	3	(Butelli et al., 2008)
Solyc01g079240	4CL6	4-coumaroyl CoA ligase	16	4	398	16	(Tohge et al., 2015)

800

801 Shown are accession numbers (1st column), gene abbreviation (2nd column), putative function (3rd
802 column), fold-change induction upon DEX application in callus after 3h (4th column), in roots after 3h
803 (5th column), in callus after 24h (6th column) and in roots after 24h (7th column) and a reference for the
804 function of the gene (8th column). Only genes for which a t-test indicates that expression upon DEX
805 induction is significantly different from non-inducing conditions (t-test n=3; P≤ 0.05) are shown. More
806 genes can be found in Supplemental Table S2.

807

808

809

810

811

812

813 REFERENCES

814

- 815 **Adrian J, Farrona S, Reimer JJ, Albani MC, Coupland G, Turck F** (2010) cis-Regulatory elements and
816 chromatin state coordinately control temporal and spatial expression of FLOWERING LOCUS T in
817 Arabidopsis. *Plant Cell* **22**: 1425-1440
- 818 **Albert NW, Davies KM, Lewis DH, Zhang H, Montefiori M, Brendolise C, Boase MR, Ngo H, Jameson
819 PE, Schwinn KE** (2014) A conserved network of transcriptional activators and repressors regulates
820 anthocyanin pigmentation in eudicots. *Plant Cell* **26**: 962-980
- 821 **Aoyama T, Chua NH** (1997) A glucocorticoid-mediated transcriptional induction system in transgenic plants.
822 *Plant J* **11**: 605-612
- 823 **Bassolino L, Zhang Y, Schoonbeek HJ, Kiferle C, Perata P, Martin C** (2013) Accumulation of anthocyanins
824 in tomato skin extends shelf life. *New Phytol* **200**: 650-655
- 825 **Bemer M, Karlova R, Ballester AR, Tikunov YM, Bovy AG, Wolters-Arts M, Rossetto Pde B, Angenent
826 GC, de Maagd RA** (2012) The tomato FRUITFULL homologs TDR4/FUL1 and MBP7/FUL2 regulate
827 ethylene-independent aspects of fruit ripening. *Plant Cell* **24**: 4437-4451
- 828 **Bernhardt C, Zhao M, Gonzalez A, Lloyd A, Schiefelbein J** (2005) The bHLH genes GL3 and EGL3
829 participate in an intercellular regulatory circuit that controls cell patterning in the Arabidopsis root
830 epidermis. *Development* **132**: 291-298
- 831 **Broun P** (2005) Transcriptional control of flavonoid biosynthesis: a complex network of conserved regulators
832 involved in multiple aspects of differentiation in Arabidopsis. *Curr Opin Plant Biol* **8**: 272-279
- 833 **Butelli E, Titta L, Giorgio M, Mock HP, Matros A, Peterek S, Schijlen EG, Hall RD, Bovy AG, Luo J,
834 Martin C** (2008) Enrichment of tomato fruit with health-promoting anthocyanins by expression of
835 select transcription factors. *Nat Biotechnol* **26**: 1301-1308
- 836 **Chanoca A, Kovinich N, Burkel B, Stecha S, Bohorquez-Restrepo A, Ueda T, Eliceiri KW, Grotewold E,
837 Otegui MS** (2015) Anthocyanin Vacuolar Inclusions Form by a Microautophagy Mechanism. *Plant Cell*
838 **27**: 2545-2559
- 839 **Chezem WR, Clay NK** (2016) Regulation of plant secondary metabolism and associated specialized cell
840 development by MYBs and bHLHs. *Phytochemistry* **131**: 26-43
- 841 **Das PK, Shin DH, Choi SB, Park YI** (2012) Sugar-hormone cross-talk in anthocyanin biosynthesis. *Mol Cells*
842 **34**: 501-507
- 843 **Davletova S, Rizhsky L, Liang H, Shengqiang Z, Oliver DJ, Coutu J, Shulaev V, Schlauch K, Mittler R**
844 (2005) Cytosolic ascorbate peroxidase 1 is a central component of the reactive oxygen gene network
845 of Arabidopsis. *Plant Cell* **17**: 268-281
- 846 **Dijken AJHv, Schluempmann H, Smeekens SCM** (2004) Arabidopsis Trehalose-6-Phosphate Synthase 1 Is
847 Essential for Normal Vegetative Growth and Transition to Flowering. *Plant Physiology* **135**: 969-977
- 848 **Frerigmann H, Berger B, Gigolashvili T** (2014) bHLH05 is an interaction partner of MYB51 and a novel
849 regulator of glucosinolate biosynthesis in Arabidopsis. *Plant Physiol* **166**: 349-369
- 850 **Girard AL, Mounet F, Lemaire-Chamley M, Gaillard C, Elmorjani K, Vivancos J, Runavot JL, Quemener
851 B, Petit J, Germain V, Rothan C, Marion D, Bakan B** (2012) Tomato GDSL1 Is Required for Cutin
852 Deposition in the Fruit Cuticle. *Plant Cell* **24**: 3119-3134
- 853 **Goldsbrough A, Belzile F, Yoder JI** (1994) Complementation of the Tomato anthocyanin without (aw) Mutant
854 Using the Dihydroflavonol 4-Reductase Gene. *Plant Physiol* **105**: 491-496
- 855 **Gomez Roldan MV, Outchkourov N, van Houwelingen A, Lammers M, Romero de la Fuente I, Ziklo N,
856 Aharoni A, Hall RD, Beekwilder J** (2014) An O-methyltransferase modifies accumulation of
857 methylated anthocyanins in seedlings of tomato. *Plant J* **80**: 695-708
- 858 **Gould KS** (2004) Nature's Swiss Army Knife: The Diverse Protective Roles of Anthocyanins in Leaves. *J Biomed*
859 *Biotechnol* **2004**: 314-320
- 860 **Grotewold E** (2006) The genetics and biochemistry of floral pigments. *Annu Rev Plant Biol* **57**: 761-780
- 861 **He J, Giusti MM** (2010) Anthocyanins: natural colorants with health-promoting properties. *Annu Rev Food Sci*
862 *Technol* **1**: 163-187
- 863 **Jonsson LM, Aarsman ME, Poulton JE, Schram AW** (1984) Properties and genetic control of four
864 methyltransferases involved in methylation of anthocyanins in flowers of *Petunia hybrida*. *Planta* **160**:
865 174-179
- 866 **Karlova R, Rosin FM, Busscher-Lange J, Parapunova V, Do PT, Fernie AR, Fraser PD, Baxter C,
867 Angenent GC, de Maagd RA** (2011) Transcriptome and metabolite profiling show that APETALA2a is
868 a major regulator of tomato fruit ripening. *Plant Cell* **23**: 923-941
- 869 **Karlova R, van Haarst JC, Maliepaard C, van de Geest H, Bovy AG, Lammers M, Angenent GC, de
870 Maagd RA** (2013) Identification of microRNA targets in tomato fruit development using high-
871 throughput sequencing and degradome analysis. *J Exp Bot* **64**: 1863-1878
- 872 **Kaufmann K, Wellmer F, Muino JM, Ferrier T, Wuest SE, Kumar V, Serrano-Mislata A, Madueno F,
873 Krajewski P, Meyerowitz EM, Angenent GC, Riechmann JL** (2010) Orchestration of floral initiation
874 by APETALA1. *Science* **328**: 85-89
- 875 **Kovinich N, Kayanja G, Chanoca A, Otegui MS, Grotewold E** (2015) Abiotic stresses induce different
876 localizations of anthocyanins in Arabidopsis. *Plant Signal Behav* **10**: e1027850
- 877 **Lashbrooke J, Adato A, Lotan O, Alkan N, Tsimbalist T, Rechav K, Fernandez-Moreno JP, Widemann
878 E, Grausem B, Pinot F, Granell A, Costa F, Aharoni A** (2015) The Tomato MIXTA-Like Transcription
879 Factor Coordinates Fruit Epidermis Conical Cell Development and Cuticular Lipid Biosynthesis and
880 Assembly. *Plant Physiol* **169**: 2553-2571

- 881 **Li Z, Omranian N, Neumetzler L, Wang T, Herter T, Usadel B, Demura T, Giavalisco P, Nikoloski Z,**
882 **Persson S** (2016) A Transcriptional and Metabolic Framework for Secondary Wall Formation in
883 Arabidopsis. *Plant Physiol* **172**: 1334-1351
- 884 **Liao D, Chen X, Chen A, Wang H, Liu J, Liu J, Gu M, Sun S, Xu G** (2015) The characterization of six auxin-
885 induced tomato GH3 genes uncovers a member, SIGH3.4, strongly responsive to arbuscular
886 mycorrhizal symbiosis. *Plant Cell Physiol* **56**: 674-687
- 887 **Lin Q, Aoyama T** (2012) Pathways for epidermal cell differentiation via the homeobox gene GLABRA2: update
888 on the roles of the classic regulator. *J Integr Plant Biol* **54**: 729-737
- 889 **Lloyd AM, Schena M, Walbot V, Davis RW** (1994) Epidermal-Cell Fate Determination in Arabidopsis -
890 Patterns Defined by a Steroid-Inducible Regulator. *Science* **266**: 436-439
- 891 **Lommen A** (2009) MetAlign: Interface-Driven, Versatile Metabolomics Tool for Hyphenated Full-Scan Mass
892 Spectrometry Data Preprocessing. *Anal Chem* **81**: 3079-3086
- 893 **Lopez-Bucio J, Cruz-Ramirez A, Herrera-Estrella L** (2003) The role of nutrient availability in regulating root
894 architecture. *Current Opinion in Plant Biology* **6**: 280-287
- 895 **Lu SY, Song T, Kosma DK, Parsons EP, Rowland O, Jenks MA** (2009) Arabidopsis CER8 encodes LONG-
896 CHAIN ACYL-COA SYNTHETASE 1 (LACS1) that has overlapping functions with LACS2 in plant wax and
897 cutin synthesis. *Plant J* **59**: 553-564
- 898 **Maloney GS, DiNapoli KT, Muday GK** (2014) The anthocyanin reduced tomato mutant demonstrates the role
899 of flavonols in tomato lateral root and root hair development. *Plant Physiol* **166**: 614-631
- 900 **Martin C, Butelli E, Petroni K, Tonelli C** (2011) How can research on plants contribute to promoting human
901 health? *Plant Cell* **23**: 1685-1699
- 902 **Martin C, Zhang Y, Tonelli C, Petroni K** (2013) Plants, diet, and health. *Annu Rev Plant Biol* **64**: 19-46
- 903 **Masucci JD, Rerie WG, Foreman DR, Zhang M, Galway ME, Marks MD, Schiefelbein JW** (1996) The
904 homeobox gene GLABRA2 is required for position-dependent cell differentiation in the root epidermis of
905 Arabidopsis thaliana. *Development* **122**: 1253-1260
- 906 **Mathews H, Clendennen SK, Caldwell CG, Liu XL, Connors K, Matheis N, Schuster DK, Menasco DJ,**
907 **Wagoner W, Lightner J, Wagner DR** (2003) Activation tagging in tomato identifies a transcriptional
908 regulator of anthocyanin biosynthesis, modification, and transport. *Plant Cell* **15**: 1689-1703
- 909 **Moco S, Bino RJ, Vorst O, Verhoeven HA, de Groot J, van Beek TA, Vervoort J, de Vos CHR** (2006) A
910 liquid chromatography-mass spectrometry-based metabolome database for tomato. *Plant Physiol* **141**:
911 1205-1218
- 912 **Morohashi K, Grotewold E** (2009) A Systems Approach Reveals Regulatory Circuitry for Arabidopsis Trichome
913 Initiation by the GL3 and GL1 Selectors. *Plos Genetics* **5**
- 914 **Munoz C, Hoffmann T, Escobar NM, Ludemann F, Botella MA, Valpuesta V, Schwab W** (2010) The
915 Strawberry Fruit Fra a Allergen Functions in Flavonoid Biosynthesis. *Molecular Plant* **3**: 113-124
- 916 **Ohashi Y, Oka A, Ruberti I, Morelli G, Aoyama T** (2002) Entopically additive expression of GLABRA2 alters
917 the frequency and spacing of trichome initiation. *Plant J* **29**: 359-369
- 918 **Outchkourov NS, Carollo CA, Gomez-Roldan V, de Vos RC, Bosch D, Hall RD, Beekwilder J** (2014)
919 Control of anthocyanin and non-flavonoid compounds by anthocyanin-regulating MYB and bHLH
920 transcription factors in Nicotiana benthamiana leaves. *Front Plant Sci* **5**: 519
- 921 **Overvoorde P, Fukaki H, Beekman T** (2010) Auxin Control of Root Development. *Cold Spring Harbor*
922 *Perspectives in Biology* **2**
- 923 **Petroni K, Tonelli C** (2011) Recent advances on the regulation of anthocyanin synthesis in reproductive
924 organs. *Plant Sci* **181**: 219-229
- 925 **Rerie WG, Feldmann KA, Marks MD** (1994) The GLABRA2 gene encodes a homeo domain protein required
926 for normal trichome development in Arabidopsis. *Genes Dev* **8**: 1388-1399
- 927 **Roldan MVG, Engel B, de Vos RCH, Vereijken P, Astola L, Groenenboom M, van de Geest H, Bovy A,**
928 **Molenaar J, van Eeuwijk F, Hall RD** (2014) Metabolomics reveals organ-specific metabolic
929 rearrangements during early tomato seedling development. *Metabolomics* **10**: 958-974
- 930 **Romero I, Tikunov Y, Bovy A** (2011) Virus-induced gene silencing in detached tomatoes and biochemical
931 effects of phytoene desaturase gene silencing. *J Plant Physiol* **168**: 1129-1135
- 932 **Roth-Walter F, Gomez-Casado C, Pacios LF, Mothes-Luksch N, Roth GA, Singer J, Diaz-Perales A,**
933 **Jensen-Jarolim E** (2014) Bet v 1 from birch pollen is a lipocalin-like protein acting as allergen only
934 when devoid of iron by promoting Th2 lymphocytes (vol 289, pg 17416, 2014). *J Biol Chem* **289**:
935 23329-23329
- 936 **Sasaki N, Nakayama T** (2015) Achievements and perspectives in biochemistry concerning anthocyanin
937 modification for blue flower coloration. *Plant Cell Physiol* **56**: 28-40
- 938 **Tohge T, Zhang Y, Peterek S, Matros A, Rallapalli G, Tandron YA, Butelli E, Kallam K, Hertkorn N,**
939 **Mock HP, Martin C, Fernie AR** (2015) Ectopic expression of snapdragon transcription factors
940 facilitates the identification of genes encoding enzymes of anthocyanin decoration in tomato. *Plant J*
941 **83**: 686-704
- 942 **Tomato Genome C** (2012) The tomato genome sequence provides insights into fleshy fruit evolution. *Nature*
943 **485**: 635-641
- 944 **Tominaga-Wada R, Nukumizu Y, Sato S, Wada T** (2013) Control of plant trichome and root-hair
945 development by a tomato (*Solanum lycopersicum*) R3 MYB transcription factor. *PLoS One* **8**: e54019
- 946 **Tominaga R, Iwata M, Sano R, Inoue K, Okada K, Wada T** (2008) Arabidopsis CAPRICE-LIKE MYB 3 (CPL3)
947 controls endoreduplication and flowering development in addition to trichome and root hair formation.
948 *Development* **135**: 1335-1345
- 949 **Tsuda T** (2012) Dietary anthocyanin-rich plants: biochemical basis and recent progress in health benefits
950 studies. *Mol Nutr Food Res* **56**: 159-170
- 951 **Van Engelen FA, Molthoff JW, Conner AJ, Nap JP, Pereira A, Stiekema WJ** (1995) pBINPLUS: An
952 improved plant transformation vector based on pBIN19. *Transgenic Res* **4**: 288-290

- 953 **Velasquez AC, Chakravarthy S, Martin GB** (2009) Virus-induced gene silencing (VIGS) in *Nicotiana*
954 *benthamiana* and tomato. *J Vis Exp*
- 955 **Xu W, Dubos C, Lepiniec L** (2015) Transcriptional control of flavonoid biosynthesis by MYB-bHLH-WDR
956 complexes. *Trends Plant Sci* **20**: 176-185
- 957 **Yeats TH, Huang WL, Chatterjee S, Viart HMF, Clausen MH, Stark RE, Rose JKC** (2014) Tomato Cutin
958 Deficient 1 (CD1) and putative orthologs comprise an ancient family of cutin synthase-like (CUS)
959 proteins that are conserved among land plants. *Plant J* **77**: 667-675
- 960 **Zafra-Stone S, Yasmin T, Bagchi M, Chatterjee A, Vinson JA, Bagchi D** (2007) Berry anthocyanins as
961 novel antioxidants in human health and disease prevention. *Mol Nutr Food Res* **51**: 675-683
- 962 **Zhang Y, Butelli E, De Stefano R, Schoonbeek HJ, Magusin A, Pagliarani C, Wellner N, Hill L, Orzaez**
963 **D, Granell A, Jones JD, Martin C** (2013) Anthocyanins double the shelf life of tomatoes by delaying
964 overripening and reducing susceptibility to gray mold. *Curr Biol* **23**: 1094-1100
- 965 **Zheng SJ, Snoeren TA, Hogewoning SW, van Loon JJ, Dicke M** (2010) Disruption of plant carotenoid
966 biosynthesis through virus-induced gene silencing affects oviposition behaviour of the butterfly *Pieris*
967 *rapae*. *New Phytol* **186**: 733-745
- 968 **Zuluaga DL, Gonzali S, Loreti E, Pucciariello C, Degl'Innocenti E, Guidi L, Alpi A, Perata P** (2008)
969 *Arabidopsis thaliana* MYB75/PAP1 transcription factor induces anthocyanin production in transgenic
970 tomato plants. *Funct Plant Biol* **35**: 606-618

971

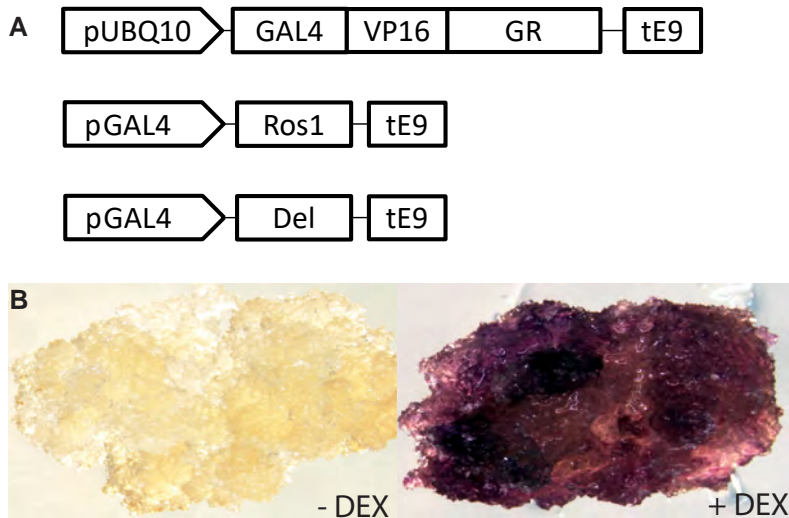


Figure 1. DEX inducible system for anthocyanin accumulation in tomato. (A) Schematic presentation of the constructs used in the study: Promoter of the *ubiquitin 10* gene from *Arabidopsis* drives the expression of a chimeric transcription factor consisting of the yeast *GAL4* DNA recognition motive-VP16 activation domain and glucocorticoid binding domain (GR). *ROS1* and *DEL* expression is controlled by a separate cassettes driven by promoter with *gal4* binding sites. (B) Representative primary callus before induction and two weeks after induction with DEX. (C) Representative primary roots of *ROS1/DEL* line 4, 5 days after DEX induction. (D) Parts of *ROS1/DEL* line 4 in soil two weeks after induction with DEX.

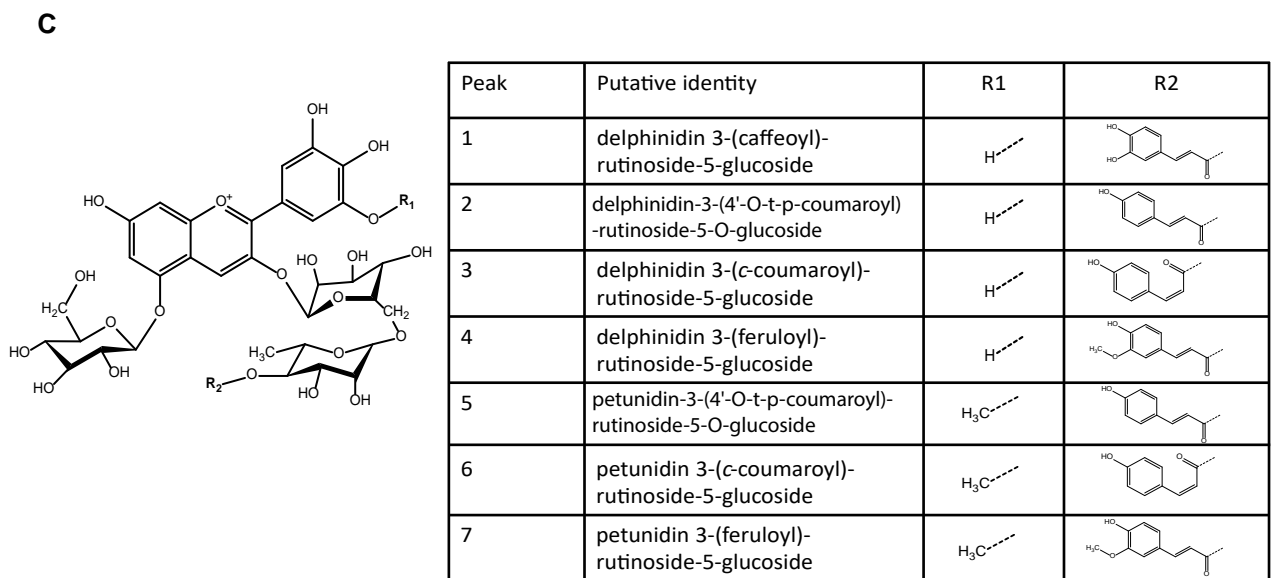
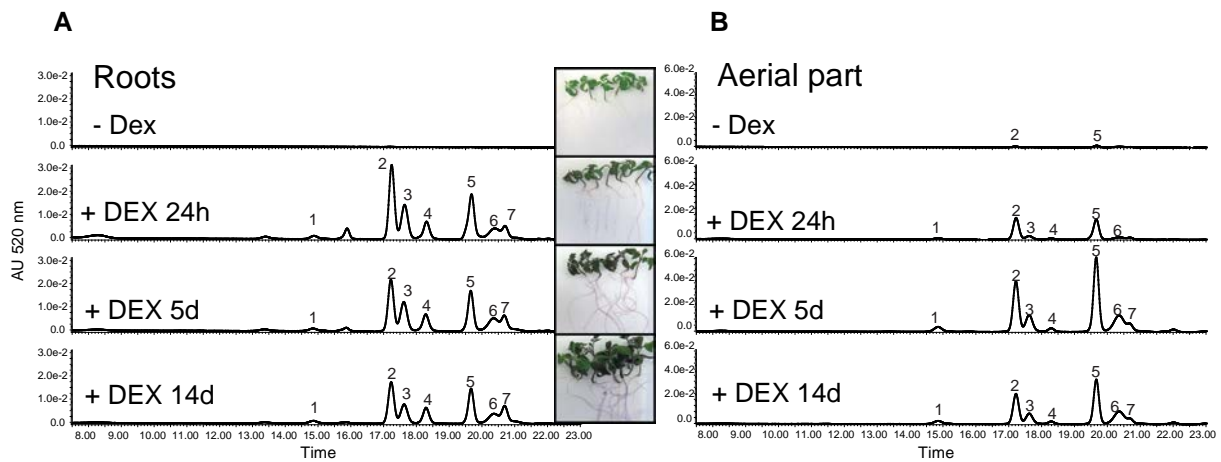


Figure 2. Metabolite analysis of ROS1/DEL activated tomato plants. Examples of chromatograms from LC-PDA-MS at 520 nm showing 7 peaks specific for anthocyanins in roots (**A**) and shoots (**B**) of tomato seedling, in the absence of DEX, or induced with DEX and sampled after 24 hours, 5 days and 14 days. (**C**) Core structure of the tomato anthocyanins. (**D**) Identity of the anthocyanins observed in (A).

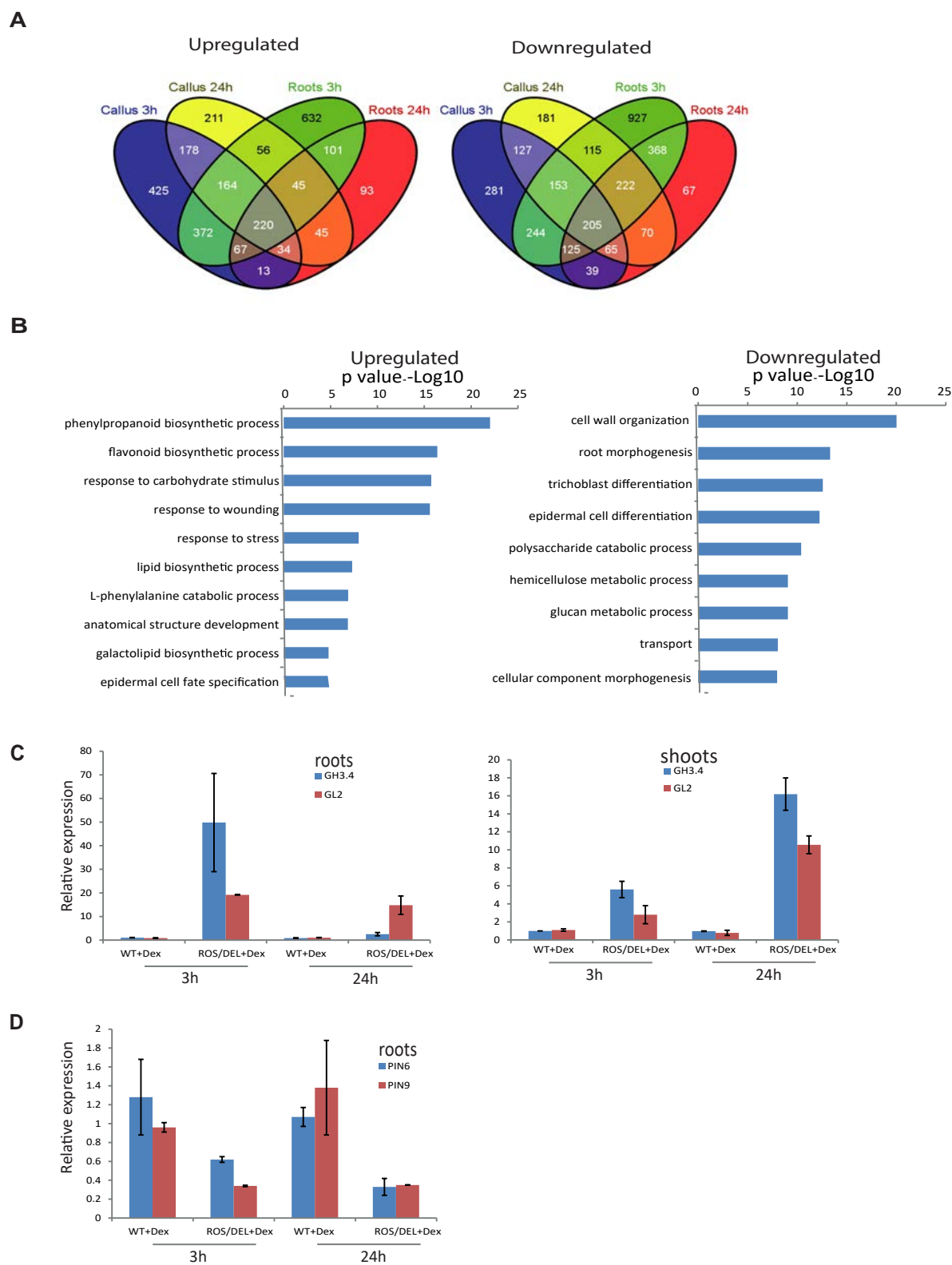


Figure 3. Gene expression profiles after DEX activation of ROS1/DEL. (A) Venn diagrams showing the overlap of up- and down-regulated genes ($p < 0.05$, fold 2) in the different tissues and time points. A core of 220 up- and 205 down-regulated genes were identified as tissue and time independent functional targets of ROS1/DEL. (B) Functional GO categories of the Up-regulated and Down-regulated genes. Bars represent p-values of GO categories which are significantly overrepresented (left) and underrepresented (right), comparing to all GO-annotated genes on the tomato genome. (C-D) Quantitative RT-PCR confirmation for *GH3.4*, *GL2* (C), *PIN6* and *PIN9* (D) gene expression ($n=4$ biological replicates; shown are mean values with standard deviations). ROS1/DEL line 4 seedlings (T4 generation) and WT seedlings were incubated with DEX for 3h and 24h. After that the roots and the shoots were analysed separately.

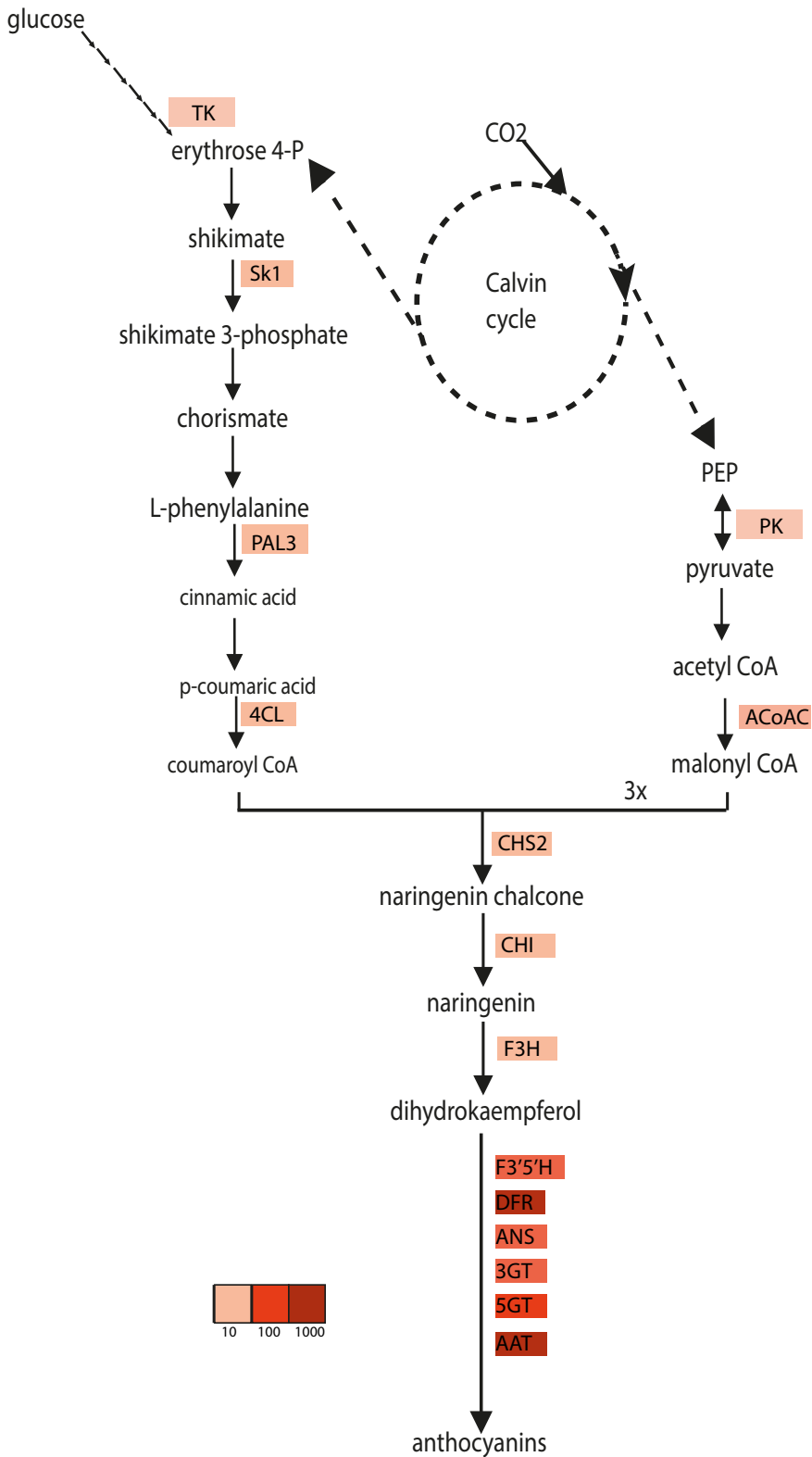
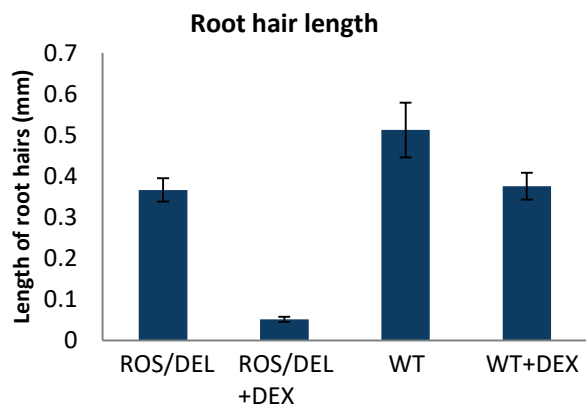


Figure 4. Genes regulated by *ROS1/DEL* in the anthocyanin pathway. Schematic overview of the anthocyanin biosynthetic pathway and the genes changing upon induction with DEX. More intense red colour indicates stronger upregulation.

A



B



C



D

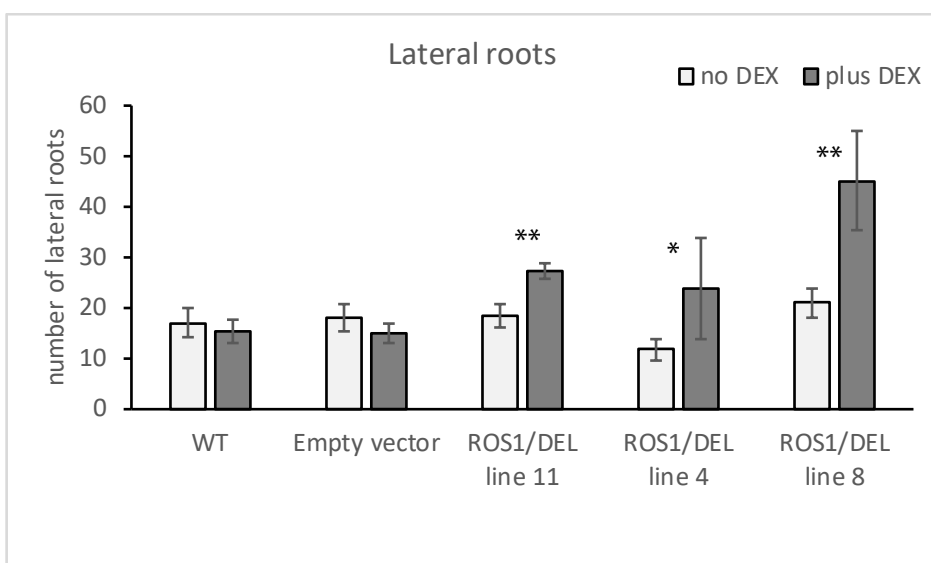


Figure 5. Phenotypic effects of *ROS1/DEL* activation on root morphology. (A) Root hair length of *ROS1/DEL* line 4 plants and WT plants in the presence and absence of DEX. Shown are mean values (n=12) and standard deviation. (B) Sectors with less purple coloration have longer root hairs. (C) Influence of *ROS1/DEL* activation on the number of lateral roots in *ROS1/DEL* line 4. Plants were transferred to media with or without DEX 5 days after germination and scored for lateral roots after 12 days of DEX induction. Black dots are placed at the end of each lateral root. (D) Number of lateral roots in the absence and presence of DEX in WT MicroTom, EV control and *ROS1/DEL* lines 4, 8 and 11. Shown are mean number of lateral roots (n=7); asterisks indicate significant differences between induced and non-induced seedlings from the same line after 12 days of growth (students t-test: *: p<0.05; **: p<0.01). Error bars represent the standard deviation.

Parsed Citations

Adrian J, Farrona S, Reimer JJ, Albani MC, Coupland G, Turck F (2010) cis-Regulatory elements and chromatin state coordinately control temporal and spatial expression of FLOWERING LOCUS T in Arabidopsis. Plant Cell 22: 1425-1440

Pubmed: [Author and Title](#)

CrossRef: [Author and Title](#)

Google Scholar: [Author Only](#) [Title Only](#) [Author and Title](#)

Albert NW, Davies KM, Lewis DH, Zhang H, Montefiori M, Brendolise C, Boase MR, Ngo H, Jameson PE, Schwinn KE (2014) A conserved network of transcriptional activators and repressors regulates anthocyanin pigmentation in eudicots. Plant Cell 26: 962-980

Pubmed: [Author and Title](#)

CrossRef: [Author and Title](#)

Google Scholar: [Author Only](#) [Title Only](#) [Author and Title](#)

Aoyama T, Chua NH (1997) A glucocorticoid-mediated transcriptional induction system in transgenic plants. Plant J 11: 605-612

Pubmed: [Author and Title](#)

CrossRef: [Author and Title](#)

Google Scholar: [Author Only](#) [Title Only](#) [Author and Title](#)

Bassolino L, Zhang Y, Schoonbeek HJ, Kiferle C, Perata P, Martin C (2013) Accumulation of anthocyanins in tomato skin extends shelf life. New Phytol 200: 650-655

Pubmed: [Author and Title](#)

CrossRef: [Author and Title](#)

Google Scholar: [Author Only](#) [Title Only](#) [Author and Title](#)

Berner M, Karlova R, Ballester AR, Tikunov YM, Bovy AG, Wolters-Arts M, Rossetto Pde B, Angenent GC, de Maagd RA (2012) The tomato FRUITFULL homologs TDR4/FUL1 and MBP7/FUL2 regulate ethylene-independent aspects of fruit ripening. Plant Cell 24: 4437-4451

Pubmed: [Author and Title](#)

CrossRef: [Author and Title](#)

Google Scholar: [Author Only](#) [Title Only](#) [Author and Title](#)

Bernhardt C, Zhao M, Gonzalez A, Lloyd A, Schiefelbein J (2005) The bHLH genes GL3 and EGL3 participate in an intercellular regulatory circuit that controls cell patterning in the Arabidopsis root epidermis. Development 132: 291-298

Pubmed: [Author and Title](#)

CrossRef: [Author and Title](#)

Google Scholar: [Author Only](#) [Title Only](#) [Author and Title](#)

Broun P (2005) Transcriptional control of flavonoid biosynthesis: a complex network of conserved regulators involved in multiple aspects of differentiation in Arabidopsis. Curr Opin Plant Biol 8: 272-279

Pubmed: [Author and Title](#)

CrossRef: [Author and Title](#)

Google Scholar: [Author Only](#) [Title Only](#) [Author and Title](#)

Butelli E, Titta L, Giorgio M, Mock HP, Matros A, Peterek S, Schijlen EG, Hall RD, Bovy AG, Luo J, Martin C (2008) Enrichment of tomato fruit with health-promoting anthocyanins by expression of select transcription factors. Nat Biotechnol 26: 1301-1308

Pubmed: [Author and Title](#)

CrossRef: [Author and Title](#)

Google Scholar: [Author Only](#) [Title Only](#) [Author and Title](#)

Chanoca A, Kovinich N, Burkel B, Stecha S, Bohorquez-Restrepo A, Ueda T, Eliceiri KW, Grotewold E, Otegui MS (2015) Anthocyanin Vacuolar Inclusions Form by a Microautophagy Mechanism. Plant Cell 27: 2545-2559

Pubmed: [Author and Title](#)

CrossRef: [Author and Title](#)

Google Scholar: [Author Only](#) [Title Only](#) [Author and Title](#)

Chezem WR, Clay NK (2016) Regulation of plant secondary metabolism and associated specialized cell development by MYBs and bHLHs. Phytochemistry 131: 26-43

Pubmed: [Author and Title](#)

CrossRef: [Author and Title](#)

Google Scholar: [Author Only](#) [Title Only](#) [Author and Title](#)

Das PK, Shin DH, Choi SB, Park YI (2012) Sugar-hormone cross-talk in anthocyanin biosynthesis. Mol Cells 34: 501-507

Pubmed: [Author and Title](#)

CrossRef: [Author and Title](#)

Google Scholar: [Author Only](#) [Title Only](#) [Author and Title](#)

Davletova S, Rizhsky L, Liang H, Shengqiang Z, Oliver DJ, Coutu J, Shulaev V, Schlauch K, Mittler R (2005) Cytosolic ascorbate peroxidase 1 is a central component of the reactive oxygen gene network of Arabidopsis. Plant Cell 17: 268-281

Pubmed: [Author and Title](#)

CrossRef: [Author and Title](#)

Google Scholar: [Author Only](#) [Title Only](#) [Author and Title](#)

Dijken AJHv, Schlupepmann H, Smeekens SCM (2004) Arabidopsis Trehalose-6-Phosphate Synthase 1 Is Essential for Normal

Downloaded from on February 13, 2018 - Published by www.plantphysiol.org

Copyright © 2017 American Society of Plant Biologists. All rights reserved.

Vegetative Growth and Transition to Flowering. Plant Physiology 135: 969-977

Pubmed: [Author and Title](#)

CrossRef: [Author and Title](#)

Google Scholar: [Author Only Title Only Author and Title](#)

Frerigmann H, Berger B, Gigolashvili T (2014) bHLH05 is an interaction partner of MYB51 and a novel regulator of glucosinolate biosynthesis in Arabidopsis. Plant Physiol 166: 349-369

Pubmed: [Author and Title](#)

CrossRef: [Author and Title](#)

Google Scholar: [Author Only Title Only Author and Title](#)

Girard AL, Mounet F, Lemaire-Chamley M, Gaillard C, Elmorjani K, Vivancos J, Runavot JL, Quemener B, Petit J, Germain V, Rothan C, Marion D, Bakan B (2012) Tomato GDSL1 Is Required for Cutin Deposition in the Fruit Cuticle. Plant Cell 24: 3119-3134

Pubmed: [Author and Title](#)

CrossRef: [Author and Title](#)

Google Scholar: [Author Only Title Only Author and Title](#)

Goldsbrough A, Belzile F, Yoder JI (1994) Complementation of the Tomato anthocyanin without (aw) Mutant Using the Dihydroflavonol 4-Reductase Gene. Plant Physiol 105: 491-496

Pubmed: [Author and Title](#)

CrossRef: [Author and Title](#)

Google Scholar: [Author Only Title Only Author and Title](#)

Gomez Roldan MV, Outchkourov N, van Houwelingen A, Lammers M, Romero de la Fuente I, Ziklo N, Aharoni A, Hall RD, Beekwilder J (2014) An O-methyltransferase modifies accumulation of methylated anthocyanins in seedlings of tomato. Plant J 80: 695-708

Pubmed: [Author and Title](#)

CrossRef: [Author and Title](#)

Google Scholar: [Author Only Title Only Author and Title](#)

Gould KS (2004) Nature's Swiss Army Knife: The Diverse Protective Roles of Anthocyanins in Leaves. J Biomed Biotechnol 2004: 314-320

Pubmed: [Author and Title](#)

CrossRef: [Author and Title](#)

Google Scholar: [Author Only Title Only Author and Title](#)

Grotewold E (2006) The genetics and biochemistry of floral pigments. Annu Rev Plant Biol 57: 761-780

Pubmed: [Author and Title](#)

CrossRef: [Author and Title](#)

Google Scholar: [Author Only Title Only Author and Title](#)

He J, Giusti MM (2010) Anthocyanins: natural colorants with health-promoting properties. Annu Rev Food Sci Technol 1: 163-187

Pubmed: [Author and Title](#)

CrossRef: [Author and Title](#)

Google Scholar: [Author Only Title Only Author and Title](#)

Jonsson LM, Aarsman ME, Poulton JE, Schram AW (1984) Properties and genetic control of four methyltransferases involved in methylation of anthocyanins in flowers of Petunia hybrida. Planta 160: 174-179

Pubmed: [Author and Title](#)

CrossRef: [Author and Title](#)

Google Scholar: [Author Only Title Only Author and Title](#)

Karlova R, Rosin FM, Busscher-Lange J, Parapunova V, Do PT, Fernie AR, Fraser PD, Baxter C, Angenent GC, de Maagd RA (2011) Transcriptome and metabolite profiling show that APETALA2a is a major regulator of tomato fruit ripening. Plant Cell 23: 923-941

Pubmed: [Author and Title](#)

CrossRef: [Author and Title](#)

Google Scholar: [Author Only Title Only Author and Title](#)

Karlova R, van Haarst JC, Maliepaard C, van de Geest H, Bovy AG, Lammers M, Angenent GC, de Maagd RA (2013) Identification of microRNA targets in tomato fruit development using high-throughput sequencing and degradome analysis. J Exp Bot 64: 1863-1878

Pubmed: [Author and Title](#)

CrossRef: [Author and Title](#)

Google Scholar: [Author Only Title Only Author and Title](#)

Kaufmann K, Wellmer F, Muino JM, Ferrier T, Wuest SE, Kumar V, Serrano-Mislata A, Madueno F, Krajewski P, Meyerowitz EM, Angenent GC, Riechmann JL (2010) Orchestration of floral initiation by APETALA1. Science 328: 85-89

Pubmed: [Author and Title](#)

CrossRef: [Author and Title](#)

Google Scholar: [Author Only Title Only Author and Title](#)

Kovinich N, Kayanja G, Chanoca A, Otegui MS, Grotewold E (2015) Abiotic stresses induce different localizations of anthocyanins in Arabidopsis. Plant Signal Behav 10: e1027850

Pubmed: [Author and Title](#)

CrossRef: [Author and Title](#)

Google Scholar: [Author Only Title Only Author and Title](#)

Lashbrooke J, Adato A, Lotan O, Nkomo M, Simbalist T, Rachav K, Fernandez-Moreno JP, Wiedemann E, Grauserm B, Pinot F, Granell A, ...

Costa F, Aharoni A (2015) The Tomato MIXTA-Like Transcription Factor Coordinates Fruit Epidermis Conical Cell Development and Cuticular Lipid Biosynthesis and Assembly. Plant Physiol 169: 2553-2571

Pubmed: [Author and Title](#)

CrossRef: [Author and Title](#)

Google Scholar: [Author Only Title Only Author and Title](#)

Li Z, Omranian N, Neumetzler L, Wang T, Herter T, Usadel B, Demura T, Giavalisco P, Nikoloski Z, Persson S (2016) A Transcriptional and Metabolic Framework for Secondary Wall Formation in Arabidopsis. Plant Physiol 172: 1334-1351

Pubmed: [Author and Title](#)

CrossRef: [Author and Title](#)

Google Scholar: [Author Only Title Only Author and Title](#)

Liao D, Chen X, Chen A, Wang H, Liu J, Liu J, Gu M, Sun S, Xu G (2015) The characterization of six auxin-induced tomato GH3 genes uncovers a member, SIGH3.4, strongly responsive to arbuscular mycorrhizal symbiosis. Plant Cell Physiol 56: 674-687

Pubmed: [Author and Title](#)

CrossRef: [Author and Title](#)

Google Scholar: [Author Only Title Only Author and Title](#)

Lin Q, Aoyama T (2012) Pathways for epidermal cell differentiation via the homeobox gene GLABRA2: update on the roles of the classic regulator. J Integr Plant Biol 54: 729-737

Pubmed: [Author and Title](#)

CrossRef: [Author and Title](#)

Google Scholar: [Author Only Title Only Author and Title](#)

Lloyd AM, Schena M, Walbot V, Davis RW (1994) Epidermal-Cell Fate Determination in Arabidopsis - Patterns Defined by a Steroid-Inducible Regulator. Science 266: 436-439

Pubmed: [Author and Title](#)

CrossRef: [Author and Title](#)

Google Scholar: [Author Only Title Only Author and Title](#)

Lommen A (2009) MetAlign: Interface-Driven, Versatile Metabolomics Tool for Hyphenated Full-Scan Mass Spectrometry Data Preprocessing. Anal Chem 81: 3079-3086

Pubmed: [Author and Title](#)

CrossRef: [Author and Title](#)

Google Scholar: [Author Only Title Only Author and Title](#)

Lopez-Bucio J, Cruz-Ramirez A, Herrera-Estrella L (2003) The role of nutrient availability in regulating root architecture. Current Opinion in Plant Biology 6: 280-287

Pubmed: [Author and Title](#)

CrossRef: [Author and Title](#)

Google Scholar: [Author Only Title Only Author and Title](#)

Lu SY, Song T, Kosma DK, Parsons EP, Rowland O, Jenks MA (2009) Arabidopsis CER8 encodes LONG-CHAIN ACYL-COA SYNTHETASE 1 (LACS1) that has overlapping functions with LACS2 in plant wax and cutin synthesis. Plant J 59: 553-564

Pubmed: [Author and Title](#)

CrossRef: [Author and Title](#)

Google Scholar: [Author Only Title Only Author and Title](#)

Maloney GS, DiNapoli KT, Muday GK (2014) The anthocyanin reduced tomato mutant demonstrates the role of flavonols in tomato lateral root and root hair development. Plant Physiol 166: 614-631

Pubmed: [Author and Title](#)

CrossRef: [Author and Title](#)

Google Scholar: [Author Only Title Only Author and Title](#)

Martin C, Butelli E, Petroni K, Tonelli C (2011) How can research on plants contribute to promoting human health? Plant Cell 23: 1685-1699

Pubmed: [Author and Title](#)

CrossRef: [Author and Title](#)

Google Scholar: [Author Only Title Only Author and Title](#)

Martin C, Zhang Y, Tonelli C, Petroni K (2013) Plants, diet, and health. Annu Rev Plant Biol 64: 19-46

Pubmed: [Author and Title](#)

CrossRef: [Author and Title](#)

Google Scholar: [Author Only Title Only Author and Title](#)

Masucci JD, Rerie WG, Foreman DR, Zhang M, Galway ME, Marks MD, Schiefelbein JW (1996) The homeobox gene GLABRA2 is required for position-dependent cell differentiation in the root epidermis of Arabidopsis thaliana. Development 122: 1253-1260

Pubmed: [Author and Title](#)

CrossRef: [Author and Title](#)

Google Scholar: [Author Only Title Only Author and Title](#)

Mathews H, Clendennen SK, Caldwell CG, Liu XL, Connors K, Matheis N, Schuster DK, Menasco DJ, Wagoner W, Lightner J, Wagner DR (2003) Activation tagging in tomato identifies a transcriptional regulator of anthocyanin biosynthesis, modification, and transport. Plant Cell 15: 1689-1703

Pubmed: [Author and Title](#)

CrossRef: [Author and Title](#)

Google Scholar: [Author Only Title Only Author and Title](#)

Moco S, Bino RJ, Vorst O, Verhoeven HA, de Groot J, van Beek TA, Vervoort J, de Vos CHR (2006) A liquid chromatography-mass spectrometry-based metabolome database for tomato. Plant Physiol 141: 1205-1218

Pubmed: [Author and Title](#)

CrossRef: [Author and Title](#)

Google Scholar: [Author Only Title Only Author and Title](#)

Morohashi K, Grotewold E (2009) A Systems Approach Reveals Regulatory Circuitry for Arabidopsis Trichome Initiation by the GL3 and GL1 Selectors. Plos Genetics 5

Pubmed: [Author and Title](#)

CrossRef: [Author and Title](#)

Google Scholar: [Author Only Title Only Author and Title](#)

Munoz C, Hoffmann T, Escobar NM, Ludemann F, Botella MA, Valpuesta V, Schwab W (2010) The Strawberry Fruit Fra a Allergen Functions in Flavonoid Biosynthesis. Molecular Plant 3: 113-124

Pubmed: [Author and Title](#)

CrossRef: [Author and Title](#)

Google Scholar: [Author Only Title Only Author and Title](#)

Ohashi Y, Oka A, Ruberti I, Morelli G, Aoyama T (2002) Entopically additive expression of GLABRA2 alters the frequency and spacing of trichome initiation. Plant J 29: 359-369

Pubmed: [Author and Title](#)

CrossRef: [Author and Title](#)

Google Scholar: [Author Only Title Only Author and Title](#)

Outchkourov NS, Carollo CA, Gomez-Roldan V, de Vos RC, Bosch D, Hall RD, Beekwilder J (2014) Control of anthocyanin and non-flavonoid compounds by anthocyanin-regulating MYB and bHLH transcription factors in Nicotiana benthamiana leaves. Front Plant Sci 5: 519

Pubmed: [Author and Title](#)

CrossRef: [Author and Title](#)

Google Scholar: [Author Only Title Only Author and Title](#)

Overvoorde P, Fukaki H, Beeckman T (2010) Auxin Control of Root Development. Cold Spring Harbor Perspectives in Biology 2

Pubmed: [Author and Title](#)

CrossRef: [Author and Title](#)

Google Scholar: [Author Only Title Only Author and Title](#)

Petroni K, Tonelli C (2011) Recent advances on the regulation of anthocyanin synthesis in reproductive organs. Plant Sci 181: 219-229

Pubmed: [Author and Title](#)

CrossRef: [Author and Title](#)

Google Scholar: [Author Only Title Only Author and Title](#)

Rerie WG, Feldmann KA, Marks MD (1994) The GLABRA2 gene encodes a homeo domain protein required for normal trichome development in Arabidopsis. Genes Dev 8: 1388-1399

Pubmed: [Author and Title](#)

CrossRef: [Author and Title](#)

Google Scholar: [Author Only Title Only Author and Title](#)

Roldan MVG, Engel B, de Vos RCH, Vereijken P, Astola L, Groenenboom M, van de Geest H, Bovy A, Molenaar J, van Eeuwijk F, Hall RD (2014) Metabolomics reveals organ-specific metabolic rearrangements during early tomato seedling development. Metabolomics 10: 958-974

Pubmed: [Author and Title](#)

CrossRef: [Author and Title](#)

Google Scholar: [Author Only Title Only Author and Title](#)

Romero I, Tikunov Y, Bovy A (2011) Virus-induced gene silencing in detached tomatoes and biochemical effects of phytoene desaturase gene silencing. J Plant Physiol 168: 1129-1135

Pubmed: [Author and Title](#)

CrossRef: [Author and Title](#)

Google Scholar: [Author Only Title Only Author and Title](#)

Roth-Walter F, Gomez-Casado C, Pacios LF, Mothes-Luksch N, Roth GA, Singer J, Diaz-Perales A, Jensen-Jarolim E (2014) Bet v 1 from birch pollen is a lipocalin-like protein acting as allergen only when devoid of iron by promoting Th2 lymphocytes (vol 289, pg 17416, 2014). J Biol Chem 289: 23329-23329

Pubmed: [Author and Title](#)

CrossRef: [Author and Title](#)

Google Scholar: [Author Only Title Only Author and Title](#)

Sasaki N, Nakayama T (2015) Achievements and perspectives in biochemistry concerning anthocyanin modification for blue flower coloration. Plant Cell Physiol 56: 28-40

Pubmed: [Author and Title](#)

CrossRef: [Author and Title](#)

Google Scholar: [Author Only Title Only Author and Title](#)

Tohge T, Zhang Y, Peterek S, Matros A, Rallapalli G, Tandron YA, Butelli E, Kallam K, Hertkorn N, Mock HP, Martin C, Fernie AR (2015) Ectopic expression of snapdragon transcription factors facilitates the identification of genes encoding enzymes of anthocyanin decoration in tomato. *Plant J* 83: 686-704

Pubmed: [Author and Title](#)

CrossRef: [Author and Title](#)

Google Scholar: [Author Only Title Only Author and Title](#)

Tomato Genome C (2012) The tomato genome sequence provides insights into fleshy fruit evolution. *Nature* 485: 635-641

Pubmed: [Author and Title](#)

CrossRef: [Author and Title](#)

Google Scholar: [Author Only Title Only Author and Title](#)

Tominaga-Wada R, Nukumizu Y, Sato S, Wada T (2013) Control of plant trichome and root-hair development by a tomato (*Solanum lycopersicum*) R3 MYB transcription factor. *PLoS One* 8: e54019

Pubmed: [Author and Title](#)

CrossRef: [Author and Title](#)

Google Scholar: [Author Only Title Only Author and Title](#)

Tominaga R, Iwata M, Sano R, Inoue K, Okada K, Wada T (2008) Arabidopsis CAPRICE-LIKE MYB 3 (CPL3) controls endoreduplication and flowering development in addition to trichome and root hair formation. *Development* 135: 1335-1345

Pubmed: [Author and Title](#)

CrossRef: [Author and Title](#)

Google Scholar: [Author Only Title Only Author and Title](#)

Tsuda T (2012) Dietary anthocyanin-rich plants: biochemical basis and recent progress in health benefits studies. *Mol Nutr Food Res* 56: 159-170

Pubmed: [Author and Title](#)

CrossRef: [Author and Title](#)

Google Scholar: [Author Only Title Only Author and Title](#)

Van Engelen FA, Molthoff JW, Conner AJ, Nap JP, Pereira A, Stiekema WJ (1995) pBINPLUS: An improved plant transformation vector based on pBIN19. *Transgenic Res* 4: 288-290

Pubmed: [Author and Title](#)

CrossRef: [Author and Title](#)

Google Scholar: [Author Only Title Only Author and Title](#)

Velasquez AC, Chakravarthy S, Martin GB (2009) Virus-induced gene silencing (VIGS) in *Nicotiana benthamiana* and tomato. *J Vis Exp*

Pubmed: [Author and Title](#)

CrossRef: [Author and Title](#)

Google Scholar: [Author Only Title Only Author and Title](#)

Xu W, Dubos C, Lepiniec L (2015) Transcriptional control of flavonoid biosynthesis by MYB-bHLH-WDR complexes. *Trends Plant Sci* 20: 176-185

Pubmed: [Author and Title](#)

CrossRef: [Author and Title](#)

Google Scholar: [Author Only Title Only Author and Title](#)

Yeats TH, Huang WL, Chatterjee S, Viart HMF, Clausen MH, Stark RE, Rose JKC (2014) Tomato Cutin Deficient 1 (CD1) and putative orthologs comprise an ancient family of cutin synthase-like (CUS) proteins that are conserved among land plants. *Plant J* 77: 667-675

Pubmed: [Author and Title](#)

CrossRef: [Author and Title](#)

Google Scholar: [Author Only Title Only Author and Title](#)

Zafra-Stone S, Yasmin T, Bagchi M, Chatterjee A, Vinson JA, Bagchi D (2007) Berry anthocyanins as novel antioxidants in human health and disease prevention. *Mol Nutr Food Res* 51: 675-683

Pubmed: [Author and Title](#)

CrossRef: [Author and Title](#)

Google Scholar: [Author Only Title Only Author and Title](#)

Zhang Y, Butelli E, De Stefano R, Schoonbeek HJ, Magusin A, Pagliarani C, Wellner N, Hill L, Orzaez D, Granell A, Jones JD, Martin C (2013) Anthocyanins double the shelf life of tomatoes by delaying overripening and reducing susceptibility to gray mold. *Curr Biol* 23: 1094-1100

Pubmed: [Author and Title](#)

CrossRef: [Author and Title](#)

Google Scholar: [Author Only Title Only Author and Title](#)

Zheng SJ, Snoeren TA, Hogewoning SW, van Loon JJ, Dicke M (2010) Disruption of plant carotenoid biosynthesis through virus-induced gene silencing affects oviposition behaviour of the butterfly *Pieris rapae*. *New Phytol* 186: 733-745

Pubmed: [Author and Title](#)

CrossRef: [Author and Title](#)

Google Scholar: [Author Only Title Only Author and Title](#)

Zuluaga DL, Gonzali S, Loreti E, Pucciariello C, Degl'Innocenti E, Guidi L, Alpi A, Perata P (2008) Arabidopsis thaliana MYB75/PAP1 transcription factor induces anthocyanin production in transgenic tomato plants. *Funct Plant Biol* 35: 606-618

Pubmed: [Author and Title](#)

CrossRef: [Author and Title](#)
Google Scholar: [Author Only](#) [Title Only](#) [Author and Title](#)